

WANL-PR(P)-009  
NASA-CR-54923



GPO PRICE \$ \_\_\_\_\_

CFSTI PRICE(S) \$ \_\_\_\_\_

Hard copy (HC) 3.00

Microfiche (MF) .75

ff 653 July 65

# DETERMINATION OF THE WELDABILITY AND ELEVATED TEMPERATURE STABILITY OF REFRACTORY METAL ALLOYS

Ninth Quarterly Report

by

G. G. Lessmann and D. R. Stoner

prepared for

National Aeronautics and Space Administration

Lewis Research Center

Space Power Systems Division

Under Contract NAS 3-2540



FACILITY FORM 602

N66 26862

(ACCESSION NUMBER)

74

(PAGES)

OR-54923

(NASA CR OR TMX OR AD NUMBER)

(THRU)

1

(CODE)

17

(CATEGORY)

**Astronuclear Laboratory**  
**Westinghouse Electric Corporation**

## NOTICE

This report was prepared as an account of Government-sponsored work. Neither the United States nor the National Aeronautics and Space Administration (NASA), nor any person acting on behalf of NASA:

- A) Makes any warranty or representation, expressed or implied, with respect to the accuracy, completeness, or usefulness of the information contained in this report, or that the use of any information apparatus, method, or process disclosed in this report may not infringe privately-owned rights; or
- B) Assumes any liabilities with respect to the use of, or for damages resulting from the use of any information, apparatus, method or process disclosed in this report.

As used above, "person acting on behalf of NASA" includes any employee or contractor of NASA, or employee of such contractor, to the extent that such employee or contractor of NASA or employee of such contractor prepares, disseminates, or provides access to, any information pursuant to his employment or contract with NASA, or his employment with such contractor.

Copies of this report can be obtained from:

National Aeronautics & Space Administration  
Office of Scientific and Technical Information  
Washington 25, D. C.  
Attention: AFSS-A

**DETERMINATION OF THE WELDABILITY AND ELEVATED  
TEMPERATURE STABILITY OF REFRACTORY METAL ALLOYS**

by

G. G. Lessmann

and

D. R. Stoner

Ninth Quarterly Report

Covering the Period

June 21, 1965 to September 20, 1965

Prepared for

**NATIONAL AERONAUTICS AND SPACE ADMINISTRATION  
Contract NAS 3-2540**

**Technical Management  
NASA-Lewis Research Center  
Cleveland, Ohio  
Space Power Systems Division  
Paul E. Moorhead**

**Astronuclear Laboratory  
Westinghouse Electric Corporation  
Pittsburgh 36, Pa.**

## FOREWORD

This report describes work accomplished under Contract NAS 3-2540 during the period June 21, 1965 to September 20, 1965. This program is being administered by R. T. Begley of the Astronuclear Laboratory, Westinghouse Electric Corporation. G. G. Lessmann and D. R. Stoner are responsible for the performance of this investigation.

Mr. P. E. Moorhead of the National Aeronautics and Space Administration is Technical Manager of this program.

TABLE OF CONTENTS

	<u>Page</u>
I. INTRODUCTION	1
II. SUMMARY	2
III. TECHNICAL PROGRAM	3
A. Weld and Base Metal Tensile Properties	3
B. Effect of Oxygen Contamination on Weldability	12
IV. FUTURE WORK	17
V. REFERENCES	18

LIST OF TABLES

	<u>Page</u>
1. Alloys Included in the Weldability and Thermal Stability Evaluations	21
2. Optimum Weld Conditions for 0.035 Inch Sheet	22
3. Compilation of Sheet Tensile Properties	23
4. One Hour Post Weld Annealing Temperatures Used on Plate Weld Tensile Specimens	27
5. Tensile Test Properties of FS-85, Uncontaminated and 500 ppm O <sub>2</sub>	28
6. Tensile Test Properties of T-111, Uncontaminated and 350 ppm O <sub>2</sub>	29
7. Tensile Test Properties of T-222, Uncontaminated and 350 ppm O <sub>2</sub>	30

LIST OF FIGURES

	<u>Page</u>
1. Room Temperature Sheet Tensile Specimen Design	31
2. Elevated Temperature Sheet Tensile Specimen Design	32
3. Elevated Temperature Tensile Strength of Annealed Base Metal and TIG Welds	33
4. Elevated Temperature Yield Strength of Annealed Base Metal and TIG Welds	34
5. Elevated Temperature Tensile Elongation of Annealed Base Metal and TIG Welds	35
6. Room Temperature Tensile Strength	36
7. Selected Metallography of Ta-10W Before and After Tensile Testing at 2400°F	37
8. T-111 Elevated Temperature Transverse Weld Tensile Fractures	38
9. T-222 Elevated Temperature Transverse Weld Tensile Fractures	39
10. Base Metal Fracture of the 2400°F B-66 Tensile Specimens	40
11. Microstructure of C-129Y, Base Metal and Transverse Weld 2400°F Tensile Specimens	41
12. Base Metal Fracture of the 2400°F Cb-752 Tensile Specimen	42
13. Weld Fracture of the 2400°F Transverse D-43 Weld Tensile Specimen	42
14. Microstructure of D-43Y Tensile Specimen Tested at 2400°F	43
15. Weld Fracture of the 2400°F FS-85 Weld Tensile Specimen	44
16. Program Outline for Contaminated Alloy Weldability Evaluation	45
17. Detailed Outline of Specimen Requirements for Oxidation Program	46
18. FS-85, Variation of Ductile-Brittle Transition Temperature with Oxygen Content	47
19. T-111, Variation of Ductile-Brittle Transition Temperature with Oxygen Content	48
20. T-222, Variation of Ductile-Brittle Transition Temperature with Oxygen Content	49

LIST OF FIGURES (Continued)

	<u>Page</u>
21. Longitudinal Bend Test Results of FS-85, Low Level O <sub>2</sub> Content	50
22. Longitudinal Bend Test Results of FS-85, High Level O <sub>2</sub> Content	51
23. Longitudinal Bend Test Results of FS-85, Preliminary Data	52
24. Longitudinal Bend Test Results of T-111, Low Level O <sub>2</sub> Content	53
25. Longitudinal Bend Test Results of T-111, High Level O <sub>2</sub> Content	54
26. Longitudinal Bend Test Results of T-111, Preliminary Data	55
27. Longitudinal Bend Test Results of T-222, Low Level O <sub>2</sub> Content	56
28. Longitudinal Bend Test Results of T-222, High Level O <sub>2</sub> Content	57
29. Longitudinal Bend Test Results of T-222, Preliminary Data	58
30. Tensile Strength Versus Temperature at Two Oxygen Levels for FS-85, T-111, and T-222	59
31. Yield Strength Versus Temperature at Two Oxygen Levels for FS-85, T-111, and T-222	60
32. Tensile Elongation Versus Temperature at Two Oxygen Levels for FS-85, T-111, and T-222	61



## I. INTRODUCTION

This is the Ninth Quarterly Progress Report describing work accomplished under Contract NAS 3-2540. The objective of this program is to determine the weldability and long time elevated temperature stability of promising refractory metal alloys in order to determine those most suitable for use in advanced alkali-metal space electric power systems. Alloys included in this investigation are listed in Table 1. A detailed discussion of the program and program objectives was presented in the First Quarterly Report. As an addition to this program, an evaluation of the effect of oxygen contamination on the weldability and thermal stability of refractory metal alloys has been undertaken. Three alloys, including T-111, T-222, and FS-85 will be evaluated. A detailed discussion and outline of this study was presented in the Seventh Quarterly Report.

Process and test controls employed throughout this program emphasize the important influence of interstitial elements on the properties of refractory metal alloys. Stringent process and test procedures are required, including continuous monitoring of the TIG weld chamber atmosphere, electron beam welding in a  $10^{-6}$  torr vacuum, aging in furnaces employing hydrocarbon free pumping systems providing pressures less than  $10^{-8}$  torr, and chemical sampling following successive stages of the evaluation for verification of these process controls.

Equipment requirements and set-up, and procedures for welding and testing, have been described in previous progress reports. Any improvements in processes, changes in procedures, or additional processes and procedures are described in this report.

## II. SUMMARY

Room temperature and elevated temperature tensile properties of the tantalum and columbium alloys were determined for both base metal and gas tungsten arc welded specimens. Tests were run at 75°F, 1800°F, 2100°F, and 2400°F. Excellent tensile weld joint efficiencies near 100% were obtained for all alloys throughout the temperature range. Tensile properties compared well with data reported by other investigators, except for D-43 which was stronger and T-222 which was weaker than anticipated.

The tensile data demonstrated that, on a density uncorrected basis, tantalum alloys were generally stronger than columbium alloys and have greater stability with increasing temperature. Within respective alloy groups, the solid solution alloys are considerably weaker than those containing reactive element solute additions which enhance strength by both dispersion and solid solution mechanisms.

An appreciation of the respective contribution of grain boundary strength and matrix strength in high temperature deformation proved important in interpreting the tensile data.<sup>32</sup> Most alloys displayed a failure mode transition between 1800°F, where fractures were primarily of the ductile shear type, and 2400°F where intergranular failures were predominant. In this respect, large weld grain sizes in either weld or base metal tended to result in lowering high temperature ductility. This was particularly apparent with Ta-10W. The yttrium containing alloys, C129Y and D43Y, exhibited extensive grain boundary separation throughout the base metal at the highest test temperature. Tensile elongation of the yttrium modified alloys was high, despite the gross separation of grain boundaries, because of small grain sizes. This advantage due to grain size could not be realized in welds, and weld tensiles failed with considerably less ductility.

The first phase of the contaminated alloy weldability study is essentially complete. In this study three alloys, T-111, T-222, and FS-85 are being compared on the basis of sensitivity to contamination by oxygen. The sensible contamination limit for this investigation was identified as 1000 ppm oxygen. At this level both the weld and base bend transition temperatures exceeded 1000°F. T-111 and FS-85 are about equivalent in oxygen sensitivity although T-111

has a definite edge because of superior initial ductility. Both of these have a tolerance of about 4000 atomic ppm (360 wt ppm in T-111 and 520 wt ppm in FS-85). Above this threshold, ductility decreases rapidly with increasing contamination. The threshold for T-222 appears to be less than 2000 atomic ppm.

Tensile results have been obtained at two oxygen levels, as received and 500 wt ppm. As had been expected, increasing oxygen content produced higher strength and less ductile behavior at all test temperatures, R.T., 1500°F, 1800°F, and 2200°F. The oxygen contamination strengthening effect on short time properties is most pronounced up to 1800°F, above which there is little difference between uncontaminated and contaminated properties, especially in FS-85. Room temperature ductility is low with contaminated T-111, and T-222 exhibiting less than 5% tensile elongation. The variation in strength and fracture location with testing temperatures indicate oxide precipitation strengthening reactions are occurring, either during the tensile test itself, as strain aging reactions, or during the preceding 50-hour diffusion anneal corresponding to the tensile testing temperature. The tensile test results of the uncontaminated specimens are comparable to the general tensile test results in this report for transverse welds in sheet specimens. Ultimate and yield strengths of T-111, T-222, and FS-85, in the two separate testing programs are similar and a difference in tensile elongation can be attributed to the respective thermal treatments; the regular program welds were post-weld annealed and the contamination program material was heat treated 50 hours at various diffusion annealing temperatures prior to welding.

### III. TECHNICAL PROGRAM

#### A. WELDING EVALUATIONS

1. Weld and Base Metal Tensile Properties - Tensile properties of the tantalum and columbium alloys were determined for base metal and tungsten arc welded specimens at room and elevated temperatures. The objective of this study was to provide a comparison of alloys based on full-range weld joint efficiencies and fracture behavior. Overall strength, as such, was not of primary concern in this evaluation since short time tensile properties cannot be extrapolated in selecting alloys for long life space power system applications, where creep strength is of primary concern.

In chronological sequence, tensile testing follows the previously reported weld parameter and post weld annealing studies. Optimum welding parameters and annealing schedules, based on weld ductility, were employed in preparing tensile specimens. This provided a realistic basis on which to compare the alloys while also providing a consistent method of sample preparation for the follow-up thermal stability phase of this program. The optimized welding parameters and post-weld anneals for 0.035-inch sheet are listed in Table 2.

Tensile tests of transverse base metal specimens and transverse TIG weld specimens were run at room temperature, 1800°F, 2100°F, and 2400°F. The base metal specimens received the same final anneal as the weld specimens and had the same orientation, i.e., rolling direction parallel to the weld direction and normal to the tensile direction. Tensile specimen designs are shown in Figures 1 and 2.

Tensile testing was conducted according to recommended Material Advisory Board procedures.<sup>1</sup> For room temperature tensiles a strain rate of 0.005 in/in/min was used through the 0.6% offset yield point, then 0.05 in/in/min to specimen fracture. At elevated temperatures a 0.05 in/in/min strain rate was used throughout the test.

Base metal specimens were tested with as-rolled and cleaned surfaces. Weld specimens were ground flat and parallel to eliminate weld contour effects on tensile behavior. This eliminated weld geometry effects and therefore provided a good metallurgical measure of weld joint efficiency. Elevated temperature specimens were either pickled just prior to testing or tested in the post-weld annealed condition in which case they had already been pickled. Testing was accomplished in the  $10^{-7}$  to low  $10^{-6}$  torr vacuum range. Specimen gage sections were wrapped in tantalum foil for additional contamination protection.

2. Tensile Test Results. The results of this investigation are described below in terms of general observations comparing alloys and alloy groups, and in terms of the individual alloy behavior. The numerous references indicated in this discussion were reviewed to compare results of this program with those reported by other investigators.

Sheet tensile test results are listed in Table 3 while Figures 3 through 6 provide a graphical comparison of alloy strength and joint efficiency. Room temperature properties of both sheet and plate are compared in Figure 6.\*

Based on ultimate strength, Figures 3 and 6, excellent joint efficiencies of nearly 100% were obtained for these alloys over the entire temperature range. Hence, all the alloys satisfy the basic objective of the tensile screening study.

This data shows that, on a density uncorrected basis, tantalum alloys are generally stronger than columbium alloys and that within respective alloy groups the solid solution strengthened alloys are considerably weaker than those which contain reactive element additions. The reactive elements, hafnium and zirconium, enhance strength both by dispersion and solid solution mechanisms. Carbide strengthening proved particularly beneficial in the case of D-43 which exhibits strength superiority among the columbium alloys at 2400°F. The experimental yttrium modification of this alloy identified as D-43Y, is considerably weaker. Interestingly, most of the columbium alloys lose uniqueness at 2400°F as demonstrated by a convergence of tensile strengths.

The tantalum alloy strength advantage is also evident in the yield strength comparison, Figure 4. Only D-43 among the columbium alloys exhibits a yield strength equivalent to that of T-222. The tantalum alloys also have an implied stability advantage since columbium alloy yield strengths fall off considerably faster with increasing temperature. The tendency for weld yield strengths to equal or exceed base metal yield strength reflects the fact that straining in transverse weld tensile tests is generally localized and does not occur uniformly throughout the gage section. Hence, one cannot infer that a true weld yield strength greater than that of the base metal was realized. Similarly, a comparison of tensile elongation behavior of

---

\*See the Eight Quarterly Report for a complete summary of the plate welding study. Post-weld anneals for plate welds are listed in Table 4.

base and weld metal is not particularly meaningful since localized yielding generally results in a lower indicated elongation in transverse weld tensiles than in base metal specimens.

Ta-10W. This is a solid solution strengthened alloy and, as such, is the weakest tantalum alloy evaluated. Surprisingly, no strength reference was located for this alloy in the recrystallized condition. Reference for stress relieved base metal,<sup>2,3,4,5</sup> indicated a higher strength at room temperature and lower strength at 2400°F than established for the recrystallized material in this program. This difference is not felt to be significant when considering the difference in final anneals. At all temperatures this alloy failed in the weld between the weld centerline and edge. Base metal ductility was good at room temperature as indicated by a chisel point failure to nearly 100% reduction in area. Although elongation increased with temperature, less reduction in area was noted between 1800°F and 2100°F due to a shift in failure mode from ductile shear to grain boundary separation. The elevated temperature grain boundary failure mode was particularly noticeable in welds which, because of a large weld grain size, failed at low total strain. This is shown dramatically in the 2400°F weld tensile fracture, Figure 7. This particular abrupt weld failure is associated primarily with Ta-10W. Other alloys which also failed by intergranular separation had smaller grain sizes and exhibited greater elongation. The large grain size of Ta-10W welds probably results from a narrow freezing range and single phase structure since it is typical of that observed in unalloyed refractory metals. The corresponding base metal specimen of Ta-10W tested at 2400°F displayed good ductility as evidenced by a chisel point mixed-mode failure and by grain elongation (uniform elongation) throughout the specimen gage section, Figure 7. This figure also shows an untested base metal structure and a typical as-tested structure in an area away from the fracture. Grain elongation, heavy working of grain boundaries and grain boundary triple point separations, are evident in the as-tested structure.

T-111. This is a high strength alloy having a joint efficiency of 94 to 100%. The tensile properties agree with those reported by the developers for this alloy.<sup>6</sup> Failures throughout the temperature range occurred in the weld rather than in the base metal. Excellent ductility was observed at room temperature with both base and weld specimens failing in

ductile shear with chisel point fractures. Respective reductions in area were approximately 100% and 80%. Ductile shear behavior persists at 1800°F, but a transition occurs with increasing temperature as evidenced by a decrease in reduction of area caused by intergranular separation and fracture before a full chisel point developed.

This tendency was more pronounced in weld failures presumably because of the larger weld grain size or perhaps differences in solute distribution. The fracture transition tendency is clearly evident in the 2100°F and 2400°F weld fractures shown in Figure 8. An incipient weld grain boundary failure is evidenced at 2100°F even though the fracture occurred by ductile shear. The 2400°F failure results primarily from weld grain boundary separation. Grain boundaries oriented most closely to the plane of maximum resolved shear stress appear to have the greatest tendency to separate. This behavior may explain a consistency of weld fracture location noted for this alloy. Grain orientation varies considerably throughout any particular weld so that one would anticipate that an area having a favorable grain boundary orientation should exist. In this respect, the actual fracture location agrees favorably with observed weld microstructures.

T-222. This is the highest strength alloy tested in this study. Joint efficiencies were good with the lowest, 88%, at 2100°F and others above 96%. Tensile properties obtained in this program were lower than expected.<sup>7,8,9</sup> A plausible explanation for this is found in stability data of T-222 reported by Ammon, Filippi, and Harrod<sup>9</sup> which showed a loss in strength of recrystallized T-222 (one hour at 3000°F) occurs after holding for 16 hours at 2000°F. A similar response may have resulted from the post weld anneal of one hour at 2400°F employed in this evaluation. Since this alloy achieves its strength in part by dispersed carbide strengthening, a reasonable possibility of an aging response of this type exists.

With the exception of the room temperature test, weld specimens failed in the weld. Base metal failures were all of the ductile shear chisel point type to about 80% reduction in area with a double shear lip finish. Weld failures were much like base metal failures through 2100°F. At 2400°F the weld fracture mode became intergranular. This transition is shown in

the photomicrographs of Figure 9. Grain boundary separations, initiated primarily at grain boundary triple points, were noted throughout the weld in the 2400°F specimen. Despite the abrupt appearance of the 2400°F weld fracture, total elongation improved over the 2100°F test indicating that good uniform elongation was obtained.

B-66. This alloy has the highest strength among the columbium alloys at 2100°F, but does not retain this advantage with increasing temperature. At 2400°F most of the columbium alloys, including B-66, have about equivalent tensile strengths. The tensile weld efficiency of this alloy is above 92% at all test temperatures. Tensile properties presented in this report are in agreement with previously reported data.<sup>10,11,12,13,14</sup>

Base tensiles displayed excellent ductility at all temperatures by failing with chisel point fractures. At room temperature the failure was slightly blunted. At 2400°F grain boundary separations were noticed near the fracture but deformation occurred primarily by ductile shear, Figure 10. Straining at 2400°F was accompanied by recrystallization resulting in a non-uniform grain size in the failed specimen. Recrystallization during testing probably accounts for the high elongation observed at 2400°F.

Weld specimens displayed a transition in tensile behavior. The room temperature specimen failed by cleavage in the weld with a reasonable elongation but with little reduction in area. At 1800°F, weld failure occurred by grain boundary separation with little reduction in area. Considerable necking in the base metal occurred at 2100°F before intergranular failure occurred in the weld. At 2400°F severe necking and failure occurred in the base metal adjacent to the heat affected zone. At both 2100°F and 2400°F the base metal experienced an overall uniform reduction in areas considerably in excess of that displayed by the weld metal.

C-129Y. This alloy has moderate strength among the columbium base alloys and a joint efficiency throughout the temperature range of 87% or greater. The tensile values obtained are 8000 to 15,000 psi below those reported for the equivalent unmodified alloy C-129. Hence,



either the post weld anneal (one hour at 2400°F) or the yttrium addition results in a reduction of strength in this alloy.<sup>15,16,17</sup>

The room temperature base metal specimen was very ductile displaying a reduction in area of nearly 100%. At 1800°F an intergranular failure occurred after about a 30% local reduction in area. At both 2100°F and 2400°F total elongation was good and intergranular failures occurred abruptly without local necking. Microstructural examination showed that gross grain boundary separation occurred throughout the gage section during testing at 2400°F, Figure 11.

Weld specimens at both room temperature and 1800°F failed in the weld by ductile shear with reductions in area of about 90%. The 2100°F and 2400°F welds had intergranular failures at the weld centerlines. A photomicrograph of the 2400°F fracture is shown in Figure 11. The fracture occurred along a single grain boundary of a peculiar centerline weld grain oriented in the welding direction. Gross grain boundary separation in this specimen was confined to the weld area although sporadic triple point openings were evident in the base metal area.

Cb-752. This alloy has moderate strength among the columbium base alloys. At room temperature the tensile weld joint efficiency was 89% while at elevated temperatures it always exceeded 100%. Tensile properties agree well with those reported<sup>2, 18, 19, 20, 21, 22,14</sup> by others. Duplex annealing is presently employed to optimize strength in this alloy.<sup>21</sup> At room temperature the duplex annealed strength is 10,000 to 15,000 psi higher than material employed in this program. At temperatures between 2000 and 2400°F this advantage is not realized and the duplex annealed strength comes within 4000 psi of results obtained in this evaluation.

Ductile shear type fractures were observed for all specimens. Elongation increased rapidly at temperatures above 1800°F. At room temperature and 1800°F, weld specimens failed in the weld whereas at 2100°F and 2400°F weld specimens failed in the base metal.

Specimen fractures were either necked down to a chisel point or necked down with a double shear lip finish. Hence, a transition at high temperature to intergranular fracture did not occur in this alloy. The 2400°F ductile shear fracture is shown in Figure 12. No evidence of grain boundary separation was observed in the weld or base metal microstructures.

D-43. This proved to be the highest strength columbium alloy above 2100°F. Weld joint tensile efficiency did not fall below 100% at any temperature. Tensile values obtained are 4000 to 8000 psi higher at elevated temperatures than those generally reported.<sup>11,22,23,24</sup> This implies that the combination of welding and post weld annealing (one hour at 2400°F) employed was entirely compatible with the as-received condition which was optimized for high temperature strength through strain induced precipitation hardening.<sup>25</sup>

The room temperature weld specimen failed in the base metal. Room temperature specimens failed with about a 40% local reduction in area with a cleavage finish. At 1800°F both base and weld failures occurred by ductile shear while at 2100°F the weld specimen failed intergranularly at the weld centerline. At 2400°F both base and weld failed primarily by grain boundary separation. The 2400°F weld specimen failed in a particularly abrupt manner with little reduction in area. This failure occurred in boundaries paralleling the direction of maximum shear stress, Figure 13. No general or incipient failures outside the local area of fracture were noticed in the sectioned 2400°F base and weld specimens.

D-43Y. This experimental alloy has a modified D-43 composition containing a minor addition of yttrium to enhance low temperature ductility. The purpose in evaluating this material was to demonstrate the feasibility of improving the bend transition ductility of D-43. Although this basic objective of improved ductility was satisfied, an extensive effort beyond the scope of this program would have been required to identify and optimize the strengthening mechanisms. As produced for this program this alloy is the weakest one evaluated except for the solid solution alloy SCb-291. Whether a strength equivalent to that of D-43 could be developed is not known. However, based on an observed bulk grain boundary separation

occurring in elevated temperature tensiles (as described below) it is doubtful that a higher strength could be realized than demonstrated by the other yttrium containing alloy, C-129Y, for which this type of fracture is typical.

At all temperatures weld specimens failed in the base metal indicating that maximum strength was not realized in producing this material. Room temperature tests displayed ductile shear behavior to about 40% local reduction in area before fracturing. At elevated temperatures fractures became progressively more abrupt. At 2400°F, the fractures were entirely intergranular with bulk grain boundary separation occurring throughout the specimen, Figure 14. The weld area of the 2400°F specimen remained in tact throughout the test although void formation was initiated at heat affected zone grain boundary triple points. Hence, even with optimized base metal structure, failure would still tend to occur at low load in the heat affected zone at a stress level not much higher than for the base metal failures observed in these tests.

FS-85. This alloy has moderate tensile strength among the columbium alloys. However, for long time applications it is more promising than is obvious from tensile data since, as reported by Titran and Hall<sup>26</sup>, its creep strength has proven to be superior to other columbium alloys. Tensile weld joint efficiencies for this alloy were above 90% at all temperatures. Tensile values obtained agree with those previously reported<sup>10,13,14</sup> except that stress relieved material<sup>14</sup> has higher strength. (All alloys in this program have been evaluated in the recrystallized condition which is generally more favorable for long time strength.)

At all temperatures the welds in this alloy fractured in preference to the base metal. At room temperature and 1800°F, failure was predominantly of the ductile shear type producing chisel point fractures except in the room temperature weld which necked locally to about a 50% reduction in area and then failed by cleavage. A transition occurred above 1800°F so that at 2400°F failures were almost completely intergranular, (Figure 15).

SCb-291. This is the lowest strength alloy evaluated. Since it is solely solid solution strengthened its primary purpose for inclusion in this program is as a reference alloy in the

thermal stability study. Like the rest of the alloys its joint efficiency is high, above 96%, throughout the temperature range. Failures were all of the ductile shear type even though grain boundary joggling was noted in welds. Only one strength reference was available<sup>27</sup> which indicated 10,000 psi higher strength values for "annealed" (presumably stress-relieved) sheet than were obtained in this evaluation.

## B. EFFECT OF OXYGEN CONTAMINATION ON WELDABILITY

The effect of oxygen contamination on the weldability and thermal stability of three selected refractory metal alloys (FS-85, T-111, and T-222) is being evaluated as an additional program to the overall weldability study. Gaseous oxidation with a low partial pressure of oxygen in helium carrier gas is being used to contaminate 0.035-inch alloy sheet. With the doping conditions employed, 800°F to 1100°F, and O<sub>2</sub> pressure of 10<sup>-1</sup> torr, an adherent oxide film is produced which is subsequently diffusion annealed at higher temperatures. The apparatus and process control are described in detail in a preceding report.<sup>28</sup> Figure 16 outlines the overall contamination program. The overall program specimen requirements are shown in Figure 17. All of the specimens have been oxygen-contaminated for Task I, a screening evaluation of the three alloys, FS-85, T-111, and T-222. The bend ductility tests have been completed and the remainder of the Task I evaluation program including tensile tests, weld restraint tests, and corroborative chemical analyses are in process.

Preliminary bend ductility results had indicated T-111 to be the least susceptible to loss in ductility due to oxygen contamination. More complete results show the same trends with T-111 and FS-85 showing little degradation in bend ductility properties up to 4000 atomic ppm oxygen. Because of its lower density, FS-85 appears better on a weight gain basis, although the small difference could be overshadowed by marked differences in in-service contamination behavior, i.e., if columbium alloys had a higher oxidation rate than tantalum alloys under operating conditions. Both our contamination runs and data reported by Inouye<sup>29</sup> indicate that columbium is more readily contaminated than tantalum at oxygen partial pressures of 4 x 10<sup>-1</sup> torr for the contamination runs and 3 x 10<sup>-7</sup> torr for Inouye's work.

Bend Test Results. Figures 18, 19, and 20 are summary curves showing the change in bend ductile-brittle transition temperature with increasing oxygen content for the three alloys. The numerous bend tests curves used to develop the summary curves are included in Figures 21 through 29.

FS-85. FS-85 shows small loss in ductility up to 500 weight ppm oxygen ( $\approx 4000$  atomic ppm oxygen). The weld bend tests have a transition temperature several hundred degrees higher than the base metal, from the as-received oxygen level of 100 ppm up to 500 ppm oxygen. The failed bend specimens showed a slightly higher incidence of fractures in the weld and heat affected zone than in the base metal. The transition from a ductile to a brittle bend generally occurred suddenly over a small temperature range and the fracture usually extended over the entire specimen. Four specimens were diffusion annealed at  $2200^{\circ}\text{F}$  with no apparent change in ductile-brittle transition temperature as compared to specimens diffusion annealed at  $1800^{\circ}\text{F}$ .

T-111. Considering the higher as-received ductile-to-brittle transition temperature of FS-85, T-111 is the most tolerant of oxygen contamination of the three alloys tested. Both T-111 and FS-85 show a sharp decrease in ductility near 4000 atomic ppm oxygen (400 weight ppm oxygen). The data obtained do not provide a reliable comparison between welded and unwelded specimens because most of the specimens were ductile at the lowest available bend test temperature,  $-320^{\circ}\text{F}$ , thus masking possible differences in ductility. Although one oxygen contamination level, 400 weight ppm oxygen, was in the area of rapid change in bend ductility behavior, the weld metal specimen was ruined during welding. The failure was a centerline tear following the weld bead and is considered to be the result of specimen geometry and welding parameters rather than an inherent material characteristic. Specimens were welded at higher (1000 weight ppm oxygen) and lower levels of oxygen contamination and no recurrence of this problem was observed. Additional specimens will be prepared in the 300-400 weight ppm oxygen range as a further check. Failures in the bend test specimens generally occurred as unarrested fractures across the entire sample with the exception of one ductile

weld tear at the 180 weight ppm oxygen level. Four specimens were diffusion annealed at 2200°F with no apparent change in ductile-brittle transition temperature compared to the standard specimens annealed at 1800°F.

T-222. T-222 has consistently shown a rapid loss in ductility at low oxygen contamination levels. At the lowest contamination level evaluated, 200 weight ppm total oxygen, ductile-brittle transition range temperature has increased from -320°F/-250°F to -150°F/+200°F. Ductile bends were not obtainable at 1000°F at oxygen levels above 400 weight ppm oxygen. In contrast to the other two alloys, the bend test failures in T-222 generally occurred in the weld and heat affected zone and were arrested in the base metal. A marked difference was observed in the unwelded bend test specimens diffusion annealed at 2200°F. These specimens produced ductile bends at the lowest test temperature, -320°F, up to 250 weight ppm oxygen, the highest oxygen contamination level so evaluated. The higher temperature diffusion annealing treatment apparently produces a different form or distribution of oxides, producing a more ductile material. Hardness traverses across the 0.035-inch cross section of T-222 had previously<sup>30</sup> shown an overall hardness decrease and a much more uniform hardness profile following the 2200°F diffusion annealing temperature. Welded specimens diffusion annealed at 2200°F, however, have the same temperature-bend ductility response as the 1800°F diffusion annealed specimens. Bend test failures in these specimens generally occurred as fractures in the weld and heat affected zone.

Tensile Test Results. Room temperature and elevated temperature (1500°F, 1800°F, and 2200°F) tensile tests have been obtained for the uncontaminated material and for the first doping level (350/500 weight ppm oxygen). The specimens were all transverse weld specimens, prepared as bead-on-plate welds with both surfaces ground flat and parallel prior to testing. The room temperature tensile tests were diffusion annealed 50 hours at 1800°F and the elevated temperature specimens were heat treated 50 hours at temperatures corresponding to their testing temperature. These thermal treatments were used to provide an application oriented thermal history. Room temperature specimens were tested as surface ground and

solvent cleaned and the elevated temperature specimens were flash pickled prior to testing in a vacuum below  $10^{-5}$  torr.

The test results are presented in curves 30, 31, and 32. As had been expected from the bend ductility results, increasing oxygen content produced stronger and less ductile behavior at all test temperatures. The oxygen contamination strengthening effect is very pronounced up to  $1800^{\circ}\text{F}$ . Tensile elongation of the contaminated alloys is low with room temperature values of less than 5% for T-111 and T-222. The uncontaminated alloys exhibit less ductility at  $1500^{\circ}\text{F}$  than at room temperature, after which the tensile elongation increases with temperature. Contaminated FS-85 shows a similar decrease in elongation at  $1500^{\circ}\text{F}$ , but contaminated T-111 and T-222 display the least ductility at room temperature. The tensile test data and photographs of the fractured gage length are shown in Tables 5, 6, and 7. A detailed analysis of fracture behavior will be deferred until the tensile test results of all five oxygen levels are available, but a general summary can be made.

Tensile Test Summary. The combination of tensile test and diffusion annealing temperatures has indicated the complexity of oxidation reactions in gettered refractory metal alloys. In reviewing these results, it must be emphasized that the oxidation reaction occurs below  $1100^{\circ}\text{F}$ , resulting in a high surface concentration of oxygen.

The lowest overall temperature cycle is seen in the  $1500^{\circ}\text{F}$  tensile specimens which are diffusion treated 50 hours at  $1500^{\circ}\text{F}$  as compared to the room temperature tensile specimens which are diffusion treated at  $1800^{\circ}\text{F}$ . Some oxide precipitation strengthening of the base metal is presumed since the contaminated specimens generally failed in the cast weld metal or apparently overaged heat affected zone. The uncontaminated alloys all failed in the base metal.

Both room temperature and  $1800^{\circ}\text{F}$  tensile specimens were diffusion annealed 50 hours at  $1800^{\circ}\text{F}$  prior to testing. The fracture locations were similar for these two groups of specimens. Contaminated specimens all failed in the weld metal and heat affected zone and uncontaminated

material, apparently not benefiting from similar oxide strengthening reactions, failed in the base metal. In the contaminated specimens, the cast weld metal and overaged heat affected zone is not strengthened by metal-oxide reactions and is weaker than the base metal. Contaminated T-111 and T-222 show no decrease in yield strength from 1500°F to 1800°F. The high strength at 1800°F could be realized by either a more uniform distribution of oxygen reaction products through the material cross section or by oxide precipitation reactions.

At 2200°F, all of the specimens showed a marked loss in strength with the base metal becoming weaker than the weld and heat affected zone. All of the specimens but one failed in the base metal with severe local deformation. One specimen, uncontaminated FS-85, failed intergranularly in the weld following appreciable base metal elongation. The oxide strengthening mechanisms are less effective at 2200°F for both the tantalum and columbium base alloys, and the overaged base metal is weaker than the weld and heat affected zone which is in the solution annealed condition. The loss in strength is most extreme in FS-85 and corresponds to the strengthening mechanism instability typical for columbium base alloys in this temperature range.<sup>31</sup>

The tensile test results of the uncontaminated specimens are comparable to the general tensile test results reported in Section III-A of this report since similar specimen design was used. The ultimate and yield strength results of T-111, T-222, and FS-85 reported for the two separate programs are similar with some difference observed in the tensile elongation. The greater elongation observed in the contaminated alloy program specimens can be attributed to different thermal histories; all material in the contaminated alloy program, including the "as-received" oxygen level, was diffusion treated 50 hours at tensile testing temperatures prior to welding.



#### IV. FUTURE WORK

Preliminary data on the thermal stability study will be obtained. This includes a comparison of a screening run at 1700°F and initial program anneals at 1500, 1800, 2100 and 2400°F.

The weldability study of the three tungsten alloys is in progress. Preliminary results from this effort will become available.

Final screening tests comparing the contamination sensitivity of FS-85, T-111 and T-222 will be completed. These will include weld restraint patch tests and tensile tests for all levels of contamination. In view of the high tolerance demonstrated by T-111, this alloy will receive a more extensive evaluation which will include 1000 hours aging at five levels of contamination and three aging temperatures. This evaluation will be initiated during the next period.

## V. REFERENCES

1. MAB-192M "Evaluation Test Methods for Refractory Metal Sheet Material".
2. 1965 Materials Selector Issue, Materials in Design Engineering.
3. Donald Peckner, "Refractory Metals Roundup", Materials in Design Engineering, October 1962.
4. DMIC Report 189, "The Engineering Properties of Tantalum and Tantalum Alloys", September 1963.
5. A. L. Feild, Jr., R. L. Ammon, A. I. Lewis, and L. S. Richardson, "Research and Development of Tantalum and Tungsten-Base Alloys", for Contract N0w-58-852-C, Final Report, Westinghouse Research Laboratories, May 26, 1961.
6. R. L. Ammon and R. T. Begley, "Pilot Production and Evaluation of Tantalum Alloy Sheet", Summary Phase Report Contract N0w-62-0656-d, WANL-PR-M-004, Westinghouse Astronuclear Laboratory, June 1963.
7. R. L. Ammon and R. T. Begley, "Pilot Production and Evaluation of Tantalum Alloy Sheet", Westinghouse Astronuclear Laboratory, WANL-PR-M-006, Fifth Quarterly Progress Report, Contract N600(19)-59762, October 1963.
8. R. L. Ammon and R. T. Begley, "Pilot Production and Evaluation of Tantalum Alloy Sheet", Summary Phase Report Part II, WANL-PR-M-009, Westinghouse Astronuclear Laboratory, July 1, 1964.
9. R. L. Ammon, A. Fillippi, D. L. Harrod, "Pilot Production and Evaluation of Tantalum Alloy Sheet", Summary Phase Report, Part III, WANL-PR-M-014, Westinghouse Astronuclear Laboratory, August 15, 1965.
10. R. A. Nadler, "Processing and Evaluation of Pre-Production Quantities of Columbium Alloy Sheet", Bureau of Naval Weapons Contract N600(19)-59546, Westinghouse Electric Corporation, Materials Manufacturing Division, January 1964.
11. R. E. Yount and D. L. Keller, "The Structural Stability of Welds in Columbium Alloys", General Electric Company, ML TDR-64-210, June 1964.
12. Westinghouse Electric Corporation, Materials Manufacturing Division Data Sheets.
13. H. L. Kohn and R. M. Curcio, "Columbium Alloy Sheet Rolling Program", Fansteel Metallurgical Corporation, Contract N0w-63-0231-C, October 1964.

14. T. L. Fullerton and J. M. Gerken, "Investigation of the Weldability of Additional Columbium Alloys", October 1963, ASD-TDR-63-843, Thompson Ramo Wooldridge, Inc.
15. Columbium and Tantalum Base Alloys for Structural and Nuclear Application, 1962 Wah Chang Corporation.
16. R. T. Torgerson, "Development and Properties of Columbium-10% Tungsten-10% Hafnium Alloy", Presented at the 1962 Fall Meeting of the Metallurgical Society of AIME.
17. DMIC Report 188, "The Engineering Properties of Columbium and Columbium Base Alloys", September 6, 1963.
18. J. G. Bewley and M. Schussler, Final Report on Development of Methods to Produce Columbium Alloy Cb-74 (Renumbered Haynes Alloy Cb-752) Sheet, ASD-TDR-63-201, Stellite Company, January 1963.
19. R. G. Baggerly and R. T. Torgerson, "Evaluation of Cb-725", The Boeing Company, Document No. D2-35105.
20. Union Carbide Corporation Data Sheet.
21. J. G. Bewley, "Strengthening of Columbium Alloy Cb-752 by Duplex-Annealing Process", Stellite Division, Union Carbide Corporation, 1965.
22. E. J. Beck and F. R. Schwartzberg, "Determination of Mechanical and Thermophysical Properties of Refractory Metals", AFML-TR-65-247, Martin Company, July 1965.
23. Technical Memorandum TM-3865-67. A Study of Welds in Columbium Alloy D-43. TRW Electrochemical Division, March 25, 1965.
24. "Product Specification, Columbium Base Alloys", Pigments Department, E. I. DuPont de Nemours Company, Inc.
25. A. L. Mincher, "Development of Optimum Manufacturing Methods for Columbium Alloy Sheet", Contract AF-33(600)39942, Interim Report IX, E. I. duPont de Nemours and Company, Inc.
26. Robert H. Titian and Robert W. Hall, "Ultrahigh-Vacuum Creep Behavior of Columbium and Tantalum Alloys at 2000<sup>o</sup> and 2200<sup>o</sup>F for Times Greater than 1000 Hours. NASA TM-X-52130, 1965.
27. Stauffer Metals Division Data Sheet for SCb-291.

28. G. G. Lessmann and D. R. Stoner, "Determination of the Weldability and Elevated Temperature Stability of Refractory Metal Alloys", Seventh Quarterly Progress Report, NASA-CR-54434, Westinghouse Electric Corporation.
29. Inouye, H., "The Contamination of Refractory Metals in Vacuums Below  $10^{-6}$  Torr", ORNL-3674. Oak Ridge National Laboratory, September 1964.
30. G. G. Lessmann and D. R. Stoner, "Determination of the Weldability and Elevated Temperature Stability of Refractory Metal Alloys", Eighth Quarterly Progress Report, NASA-CR-54723. Westinghouse Electric Corporation.
31. R. T. Begley, R. L. Ammon, R. Stickler, "Development of Niobium Base Alloys", WADC-TR-57-344, Part VI, February 1963. Westinghouse Electric Corporation.
32. R. T. Begley, J. L. Godshall, "Some Observations on the Role of Grain Boundaries in High Temperature Deformation and Fracture of Refractory Metals", Presented at the AIME Symposium on the Physical Metallurgy of Refractory Metals, French Lick, Indiana, October 3-5, 1965, WANL-SP-012, January 15, 1966.

**TABLE 1 - Alloys Included in the Weldability and Thermal Stability Evaluations**

<u>Alloy</u>	<u>Nominal Composition Weight Percent</u>
AS-55	Cb-5W-1Zr-0.2Y-0.06C
B-66	Cb-5Mo-5V-1Zr
C-129Y	Cb-10W-10Hf+Y
Cb-752	Cb-10W-2.5Zr
D-43	Cb-10W-1Zr-0.1C
FS-85	Cb-27Ta-10W-1Zr
SCb-291	Cb-10W-10Ta
D43 + Y	Cb-10W-1Zr-0.1C+Y
T-111	Ta-8W-2Hf
T-222	Ta-9.6W-2.4Hf-0.01C
Ta-10W	Ta-10W
W-25 Re	W-25Re
W	Unalloyed
Sylvania "A"*	W-0.5Hf-0.02C

\* NOTE: All alloys from arc-cast and/or electron beam melted material except Sylvania "A"

**TABLE 2 - Optimized Weld Conditions**

Alloy	Process	Parameters (1)	One Hour Post Weld Anneal Temp., °F	Weld Width Top/Bottom (inches)	BDBTT, °F <sup>(2)</sup>	
					Long. Bends	Trans. Bends
Ta-10W	TIG	7.5-1/4-118	None	.190/.180	<-320	<-320
	EB	15-1/2-4.5	None	.049/.034	<-320	<-320
T-111	TIG	15-3/8-115	2400°F	.195/.189	<-320	<-320
	EB	15-1/2-3.8	2400°F	.038/.027	<-320	<-320
T-222	TIG	30-1/4-190	2400°F	.180/.159	<-320	<-320
	EB	15-1/2-3.8	2400°F	.039/.026	<-320	<-320
B-66	TIG	15-3/8-86	None	.190/.180	0	+75
	EB	25-3/16-3.2	1900°F	.036/.024	-225	-175
C-129Y	TIG	30-3/8-110	2400°F	.180/.130	-200	-225
	EB	50-1/2-4.1	2200°F	.040/.026	-250	-250
Cb-752	TIG	30-3/8-87	2200°F	.129/.090	-75	0
	EB	15-3/16-3.3	2400°F	.036/.017	-200	-200
D-43	TIG	30-3/8-114	2400°F	.159/.143	+100	0 <sup>(3)</sup>
	EB	50-1/2-4.4	2400°F	.040/.027	-225	-225
D-43Y	TIG	15-3/8-83	2400°F	.165/.150	-175	-250
	EB	50-1/2-4.0	2400°F	.036/.022	-250	<-300
FS-85	TIG	15-3/8-90	2400°F	.204/.195	-175	-175
	EB	50-3/16-4.4	2200°F	.038/.026	-200	-200
SCb-291	TIG	15-1/4-83	2200°F	.160/.150	-275	-275
	EB	50-1/2-4.4	None	.038/.027	<-320	-250

(1) For TIG Welds: Speed (ipm) - Clamp Spacing (in.) - Amperes  
 For EB Welds: Speed (ipm) - Clamp Spacing (in.) - Milliampères  
 (All EB welds with 60~ $\mu$ , 0.050 inch longitudinal deflection and  
 150 KV beam voltage)

(2) BDBTT  $\approx$  Bend Ductile Brittle Transition Temperature at 1t Bend Radius Except  
 FS-85 EB Welds at 2t Bend Radius.

(3) Probable Value (Determined Value  $\leq$  -125°F)

**TABLE 3 - Compilation of Sheet Tensile Properties**

Alloy	Test Temp. (°F)	Specimen Type	Pre-Test 1 Hr. Anneal Temp. (°F)	Ultimate Strength psi x 10 <sup>-3</sup>	0.2% Offset Yield Strength psi x 10 <sup>-3</sup>	Elongation (%)	Weld Joint* Efficiency (%)	Fracture Location
Ta-10W	R. T.	Base	None	84.4	71.5	29	--	--
	R. T.	Weld	None	81.4	69.9	9	97	Weld
	1800	Base	None	42.3	24.5	33	--	--
	1800	Weld	None	38.2	23.9	8	90	Weld
	2100	Base	None	33.7	17.6	42	--	--
	2100	Weld	None	29.5	19.7	5	88	Weld
	2400	Base	None	25.3	20.9	67	--	--
	2400	Weld	None	22.8	14.6	4	90	Weld
T-111	R. T.	Base	2400	89.2	83.2	16	--	--
	R. T.	Weld	2400	92.0	82.5	14	102	Weld
	1800	Base	2400	61.3	34.6	14	--	--
	1800	Weld	2400	58.2	32.3	10	95	Weld
	2100	Base	2400	52.2	29.2	20	--	--
	2100	Weld	2400	49.0	30.2	14	94	Weld
	2400	Base	2400	38.9	23.4	32	--	--
	2400	Weld	2400	37.7	23.9	10	97	Weld
T-222	R. T.	Base	2400	88.0	80.1	18	--	--
	R. T.	Weld	2400	90.1	83.2	14	101	Base
	1800	Base	2400	62.8	33.9	10	--	--
	1800	Weld	2400	60.3	36.0	6	96	Weld
	2100	Base	2400	57.3	31.8	14	--	--
	2100	Weld	2400	52.7	32.9	7	88	Weld
	2400	Base	2400	39.9	27.9	20	--	--
	2400	Weld	2400	40.9	28.7	12	102	Weld

TABLE 3 - Compilation of Sheet Tensile Properties  
(Continued)

Alloy	Test Temp. (°F)	Specimen Type	Pre-Test 1 Hr. Anneal Temp. (°F)	Ultimate Strength psi x 10 <sup>-3</sup>	0.2% Offset Yield Strength psi x 10 <sup>-3</sup>	Elongation (%)	Weld Joint Efficiency (%)	Fracture Location
B-66	R. T.	Base	None	104.73	79.88	22.5	--	--
	R. T.	Weld	None	100.92	81.04	9	97	Weld
	1800	Base	None	66.9	39.0	48	--	--
	1800	Weld	None	61.5	43.5	6	92	Weld
	2100	Base	None	39.7	29.1	69	--	--
	2100	Weld	None	42.3	33.2	13	103	Weld
	2400	Base	None	23.1	21.1	106	--	--
	2400	Weld	None	22.8	20.0	67	99	Base
C-129Y	R. T.	Base	2400	85.97	72.06	26.5	--	--
	R. T.	Weld	2400	74.93	66.54	5.5	87	Weld
	1800	Base	2400	51.7	31.8	27	--	--
	1800	Weld	2400	45.9	30.2	7	89	Weld
	2100	Base	2400	37.6	25.7	26	--	--
	2100	Weld	2400	36.6	28.8	6	98	Weld
	2400	Base	2400	24.7	20.1	84	--	--
	2400	Weld	2400	24.6	20.0	8	100	Weld
Cb-752	R. T.	Base	2200	73.10	55.50	27	--	--
	R. T.	Weld	2200	64.80	48.80	12.5	89	Weld
	1800	Base	2200	47.1	27.1	24	--	--
	1800	Weld	2200	50.6	28.2	13	104	Weld
	2100	Base	2200	34.6	22.6	40	--	--
	2100	Weld	2200	36.6	24.6	36	103	Base
	2400	Base	2200	22.7	15.6	72	--	--
	2400	Weld	2200	23.7	19.7	66	102	Base



**TABLE 3 - Compilation of Sheet Tensile Properties  
(Continued)**

Alloy	Test Temp. (°F)	Specimen Type	Pre-Test 1 Hr. Anneal Temp. (°F)	Ultimate Strength psi x 10 <sup>-3</sup>	0.2% Offset Yield Strength psi x 10 <sup>-3</sup>	Elongation (%)	Weld Joint* Efficiency (%)	Fracture Location
D-43	R. T.	Base	2400	90.21	62.15	19.5	--	--
	R. T.	Weld	2400	90.26	63.75	18.0	100	Base
	1800	Base	2400	54.9	39.0	14	--	--
	1800	Weld	2400	55.6	42.1	8	101	Weld
	2100	Base	2400	43.3	33.7	16	--	--
	2100	Weld	2400	43.6	38.6	9	100	Weld
	2400	Base	2400	32.7	24.7	21	--	--
	2400	Weld	2400	32.6	27.7	6	100	Weld
D-43Y	R. T.	Base	2400	62.75	39.57	24.0	--	--
	R. T.	Weld	2400	70.03	42.35	22.5	112	Base
	1800	Base	2400	37.3	31.3	27	--	--
	1800	Weld	2400	37.5	21.2	20	100	Base
	2100	Base	2400	27.8	15.3	19	--	--
	2100	Weld	2400	26.6	18.7	38	95	Base
	2400	Base	2400	16.9	13.8	18	--	--
	2400	Weld	2400	17.7	15.4	18	102	Base
FS-85	R. T.	Base	2400	83.10	67.60	22.5	--	--
	R. T.	Weld	2400	78.60	61.90	10	95	Weld
	1800	Base	2400	44.6	21.7	20	--	--
	1800	Weld	2400	40.4	22.1	8	90	Weld
	2100	Base	2400	34.5	21.9	30	--	--
	2100	Weld	2400	33.1	20.6	8	96	Weld
	2400	Base	2400	22.7	15.0	51	--	--
	2400	Weld	2400	23.4	15.4	12	102	Weld

TABLE 3 - Compilation of Sheet Tensile Properties  
(Continued)









Alloy	Test Temp. (°F)	Specimen Type	Pre-Test 1 Hr. Anneal Temp. (°F)	Ultimate Strength psi x 10 <sup>-3</sup>	0.2% Offset Yield Strength psi x 10 <sup>-3</sup>	Elongation (%)	Weld Joint <sup>*</sup> Efficiency (%)	Fracture Location
SCb-291	R. T.	Base	2200	59.57	47.53	23.5	--	--
	R. T.	Weld	2200	57.20	45.90	9	96	Weld
	1800	Base	2200	20.9	12.3	46	--	--
	1800	Weld	2200	20.4	12.1	15	98	Weld
	2100	Base	2200	14.8	8.0	46	--	--
	2100	Weld	2200	16.0	10.8	43	108	Base
	2400	Base	2200	12.7	7.7	68	--	--
	2400	Weld	2200	12.6	7.5	50	99	Base

\* NOTE: Weld specimen surfaces ground flat and parallel to avoid surface contour effects providing a truer metallurgical joint efficiency.

**TABLE 4 - One Hour Post Weld Annealing Temperatures Used  
on Plate Weld Tensile Specimens**









Ta-10W	None
T-111	2400°F
T-222	2400°F
B-66	1900°F
C-129Y	2400°F
Cb-752	2200°F
D-43	2400°F
FS-85	2400°F
SCb-291	1900°F

TABLE 5. Tensile Test Properties of FS-85, Uncontaminated and 500 Ppm O<sub>2</sub>

Specimen	O <sub>2</sub> Level ppm	50-Hr. Diffusion Temp. F°	Test Temp. F°	Yield Stress 0.2% Offset Psi x 10 <sup>3</sup>	Ultimate Stress Psi x 10 <sup>3</sup>	Elongation %	Fracture Location	Fracture Description
C3CU-1	100 <sup>1</sup>	1800	R.T.	64.3	84.5	20.0	Weld	
C3CI-4	500	1800	R.T.	76.6	94.8	9.0	HAZ <sup>2</sup>	
C3CU-3	100 <sup>1</sup>	1500	1500	31.4	52.1	16.0	Base	
C3CI-1	500	1500	1500	47.2	60.0	5.0	Weld	
C3CU-2	100 <sup>1</sup>	1800	1800	28.9	42.9	17.0	Base	
C3CI-3	500	1800	1800	42.4	52.8	8.0	HAZ <sup>2</sup>	
C3CU-4	100 <sup>1</sup>	2200	2200	22.4	29.2	20.0	Weld	
C3CI-2	500	2200	2200	23.7	29.3	27.0	Base	









(1) Uncontaminated  
(2) Heat Affected Zone

**TABLE 6. Tensile Test Properties of T-111, Uncontaminated and 350 PPM O<sub>2</sub>**

Specimen	O <sub>2</sub> Level PPM	50-Hr. Diffusion Temp. °F	Test Temp. °F	Yield Stress 0.2% Offset Psi x 10 <sup>3</sup>	Ultimate Stress Psi x 10 <sup>3</sup>	Elongation %	Fracture Location	Fracture Description
TICU-3	40 <sup>1</sup>	1800	R. T.	75.3	86.6	19.5	Base	
TICI-3	350	1800	R. T.	88.5	99.0	3.5	HAZ <sup>2</sup>	
TICU-1	40 <sup>1</sup>	1500	1500	38.8	64.0	14.0	Base	
TICI-2	350	1500	1500	50.6	70.6	8.0	Weld	
TICU-4	40 <sup>1</sup>	1800	1800	33.9	57.3	15.0	Base	
TICI-4	350	1800	1800	51.6	66.3	7.0	HAZ <sup>2</sup>	
TICU-2	40 <sup>1</sup>	2200	2200	29.0	42.4	24.0	Base	
TICI-1	350	2200	2200	35.5	46.6	22.0	Base	

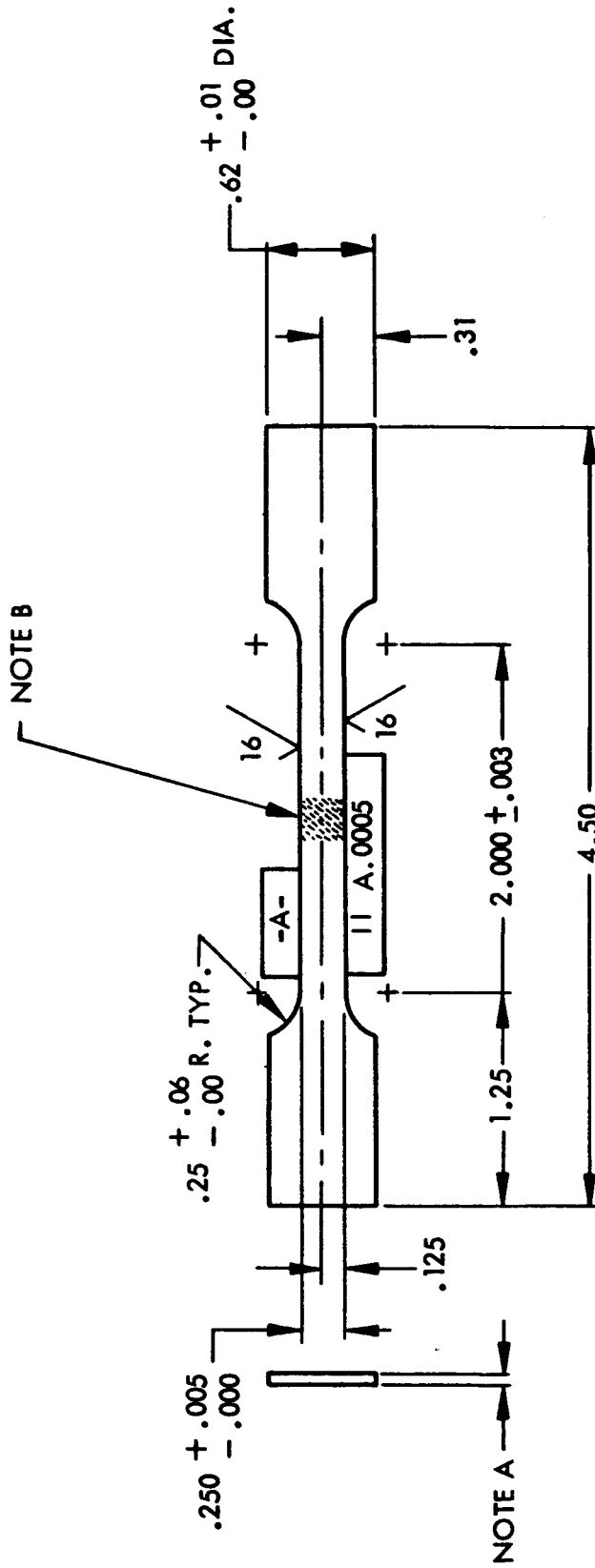
(1) Uncontaminated  
(2) Heat Affected Zone

**TABLE 7. Tensile Test Properties of T-222, Uncontaminated and 350 PPM O<sub>2</sub>**

Specimen	O <sub>2</sub> Level PPM	50-Hr. Diffusion Temp. °F	Test Temp. °F	Yield Stress 0.2% Offset Psi x 10 <sup>3</sup>	Ultimate Stress Psi x 10 <sup>3</sup>	Elongation %	Fracture Location	Fracture Description
T3CU-2	85 <sup>1</sup>	1800	R. T.	73.8	85.2	12.0	Base	
T3CI-2	350	1800	R. T.	98.7	106.6	3.0	HAZ <sup>2</sup>	
T3CU-1	85 <sup>1</sup>	1500	1500	40.3	61.5	10.0	Base	
T3CI-4	350	1500	1500	49.6	75.5	11.0	Base	
T3CU-4	85 <sup>1</sup>	1800	1800	39.4	61.6	10.0	Base	
T3CI-3	350	1800	1800	60.2	75.1	6.0	Weld	
T3CU-3	85 <sup>1</sup>	2200	2200	35.2	48.9	15.0	Base	
T3CI-1	350	2200	2200	44.0	53.8	13.0	Base	

(1) Uncontaminated

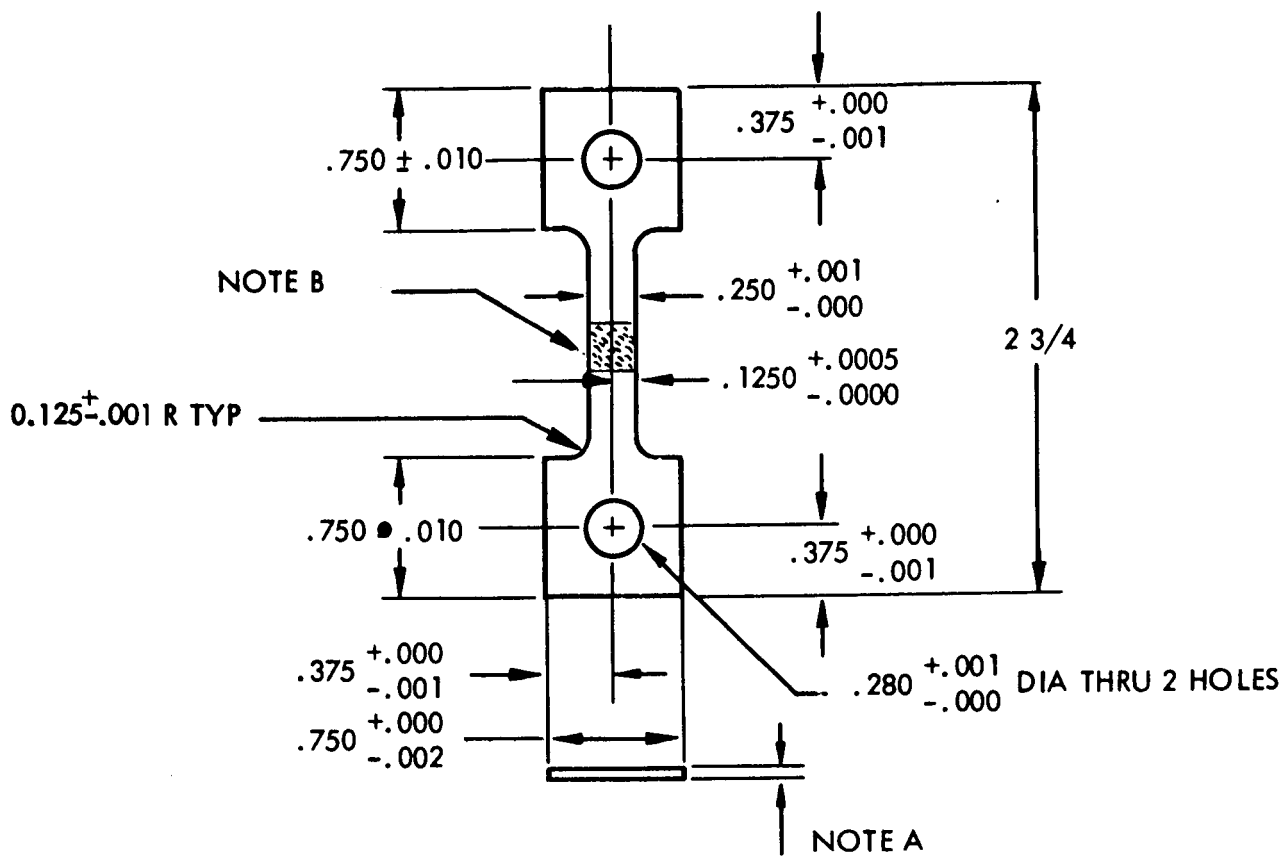
(2) Heat Affected Zone



- NOTES:**
- A. AS RECEIVED SHEET THICKNESS, EXCEPT WELDED SPECIMENS WHICH ARE GROUND TO BE FLAT AND PARALLEL WITHIN .0005
  - B. WELD LOCATION FOR WELD SPECIMENS - CENTER IN GAGE SECTION
  - C. DIMENSIONAL TOLERANCES UNLESS OTHERWISE NOTED: TWO PLACE DECIMALS -  $\pm .02$  THREE PLACE DECIMALS -  $\pm .005$

603897-1 B

FIGURE 1 - Room Temperature Sheet Tensile Specimen Design

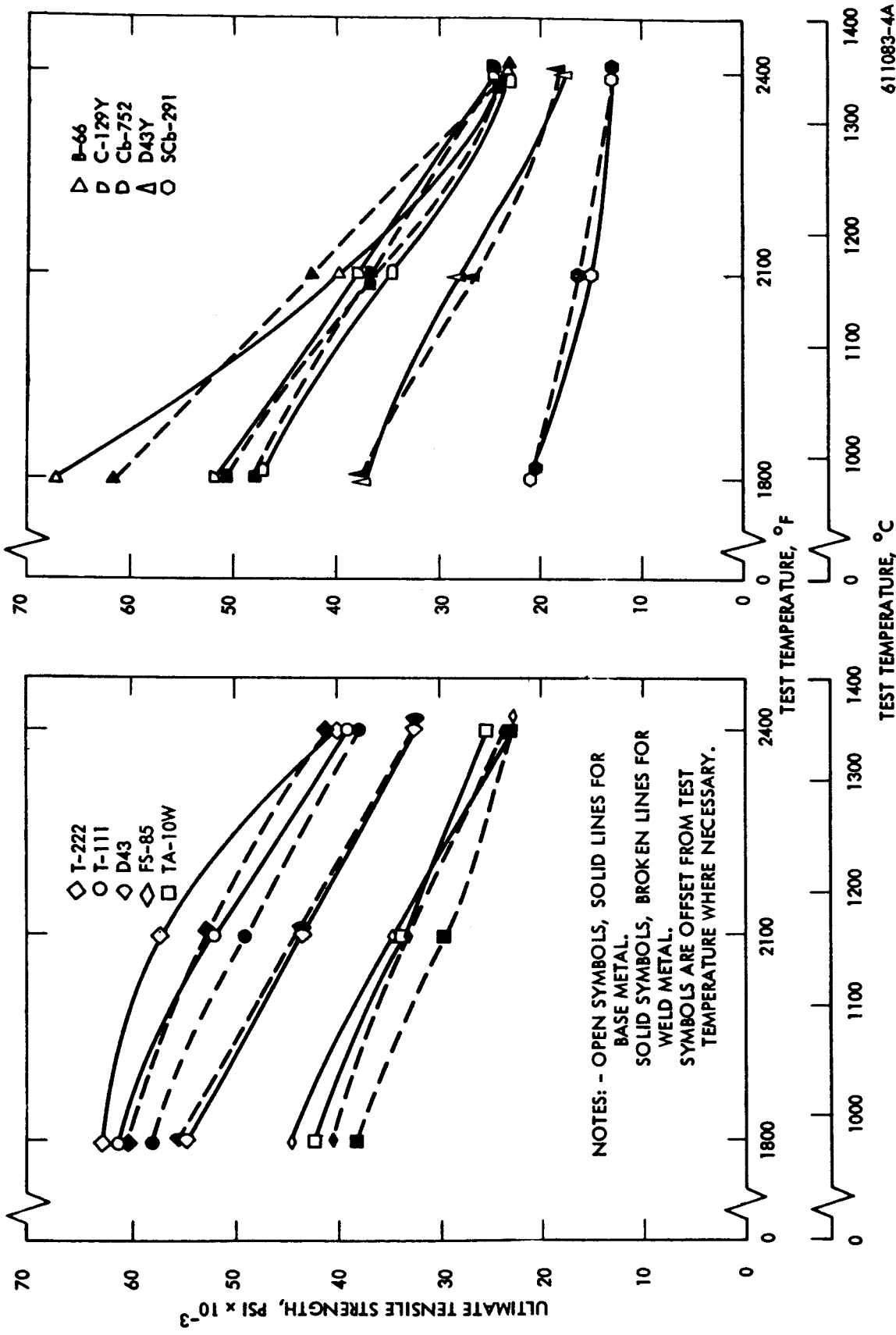


NOTES:

- A. AS RECEIVED SHEET THICKNESS EXCEPT WELDED SPECIMENS WHICH ARE GROUND TO BE FLAT AND PARALLEL WITHIN 0.0005
- B. WELD LOCATION FOR WELD SPECIMENS - CENTER IN GAGE SECTION

FIGURE 2 - Elevated Temperature Sheet Tensile Specimen Design





611083-4A

FIGURE 3 - Elevated Temperature Tensile Strength of Annealed Base Metal and TIG Welds

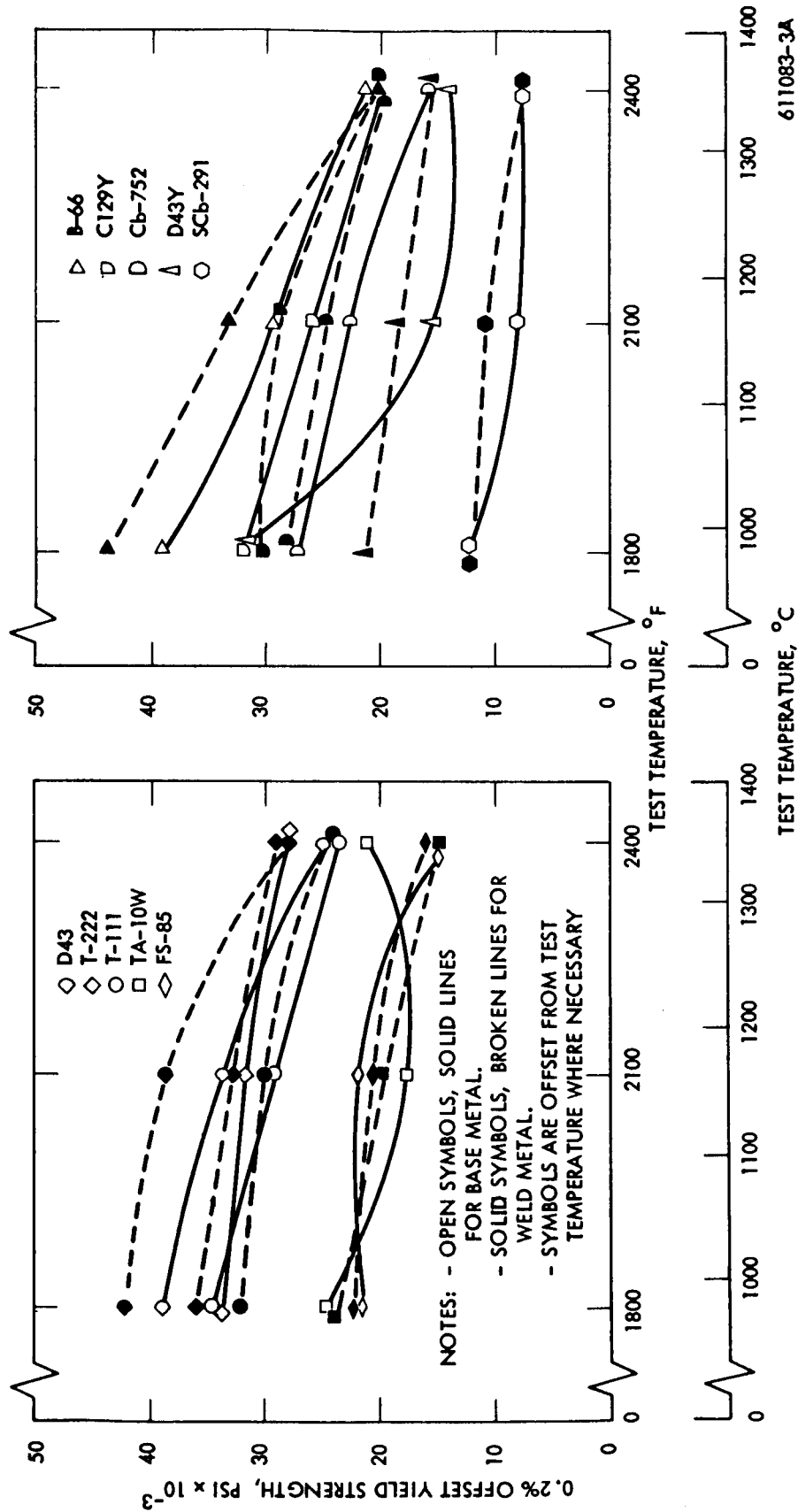
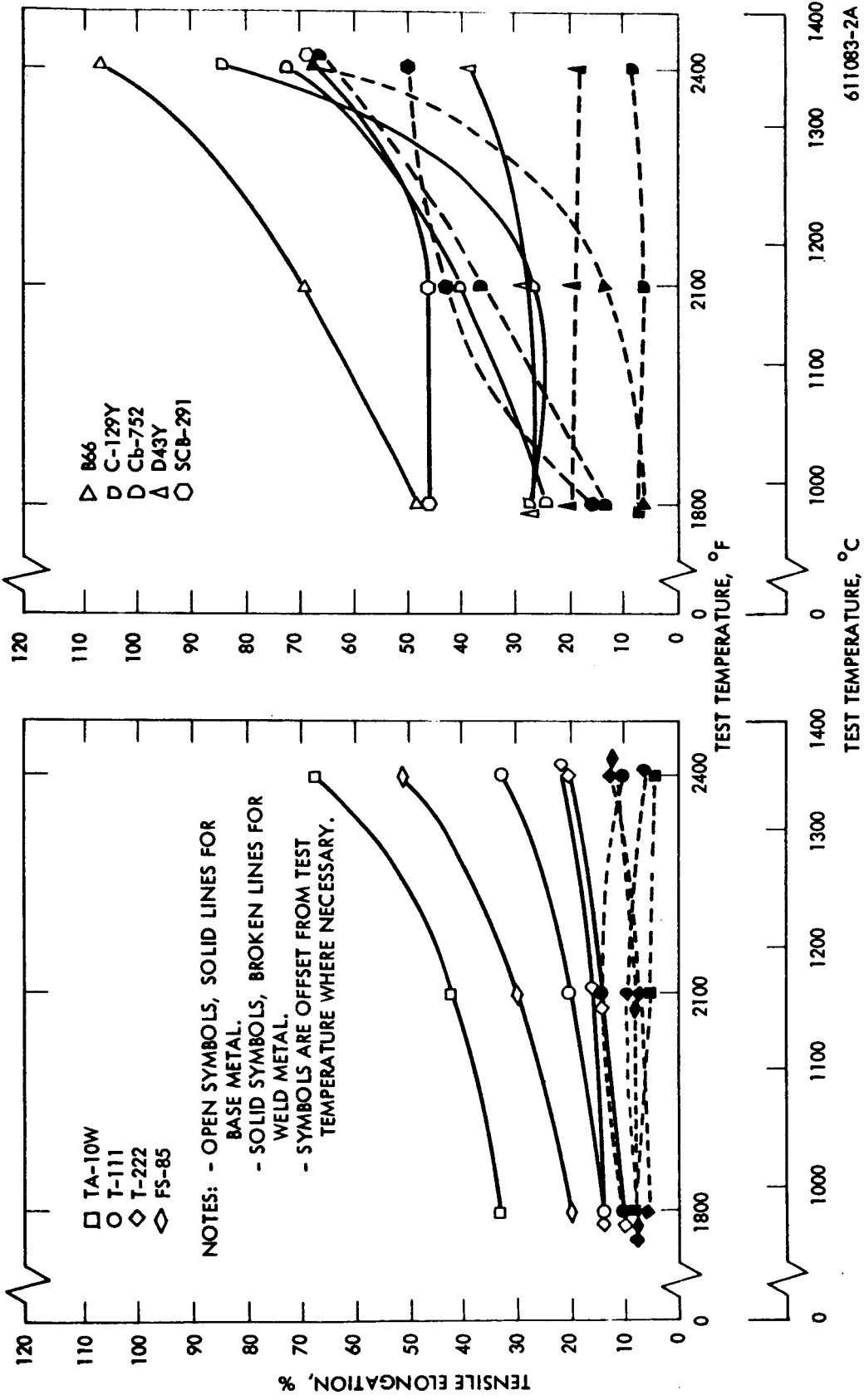


FIGURE 4 - Elevated Temperature Yield Strength of Annealed Base Metal and TIG Welds



611083-2A

FIGURE 5 - Elevated Temperature Tensile Elongation of Annealed Base Metal and TIG Welds

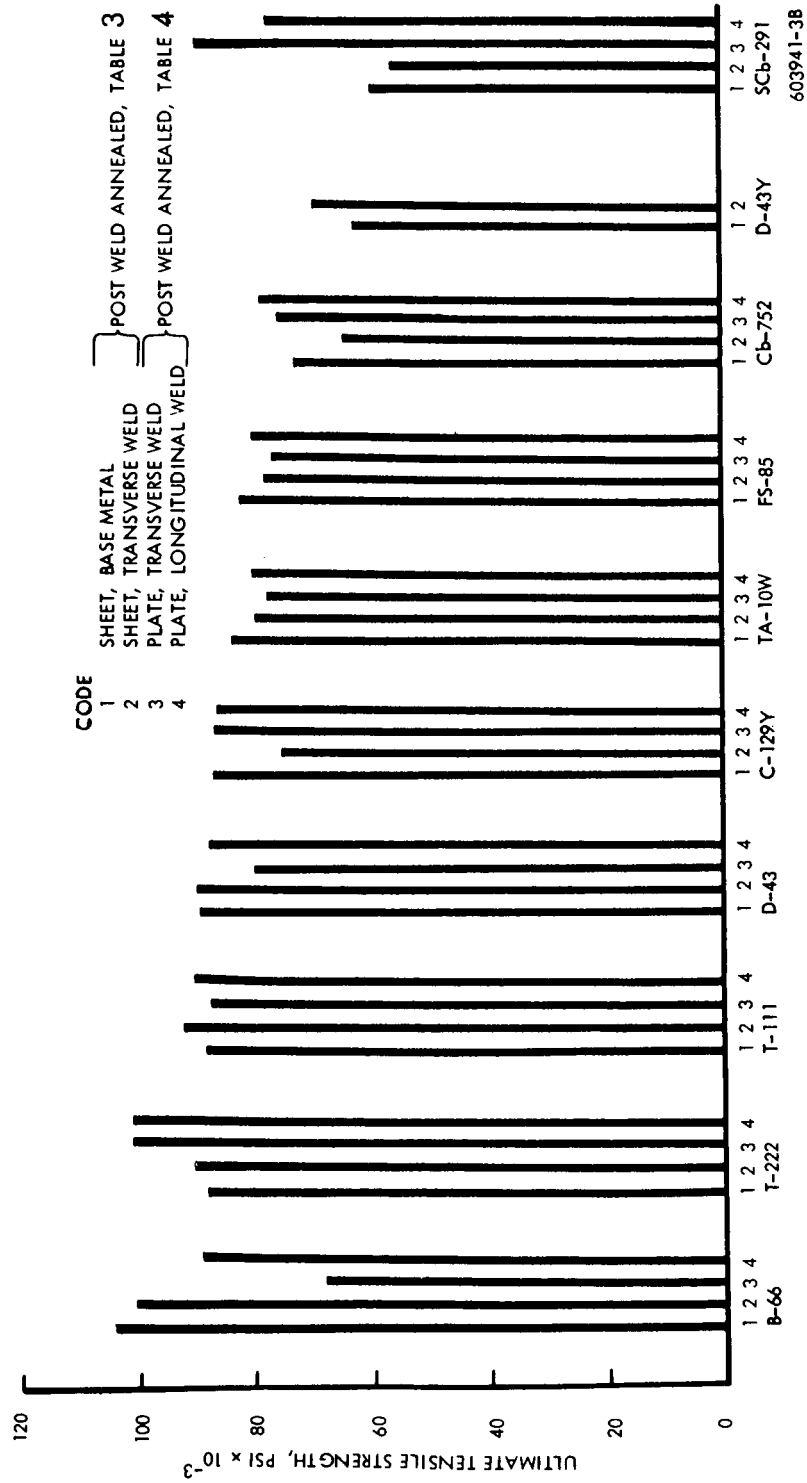
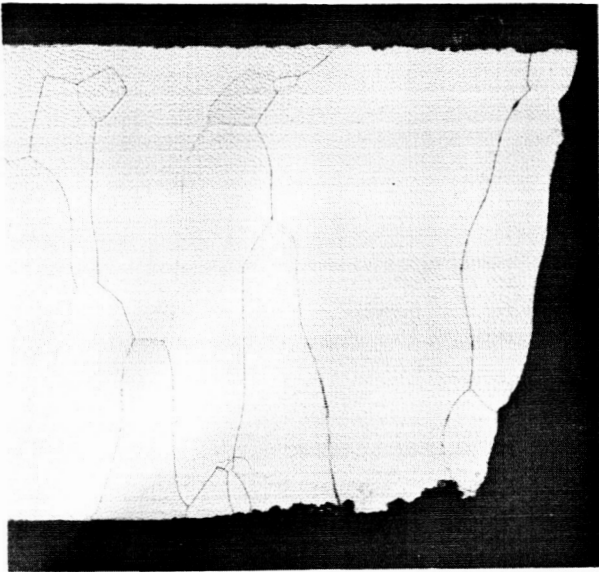
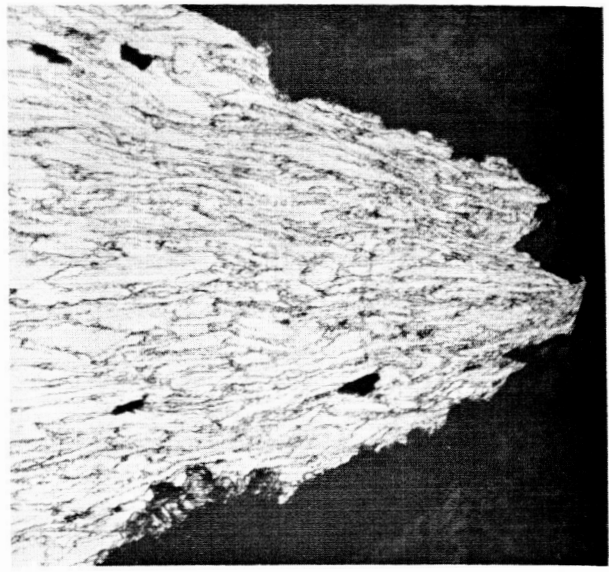


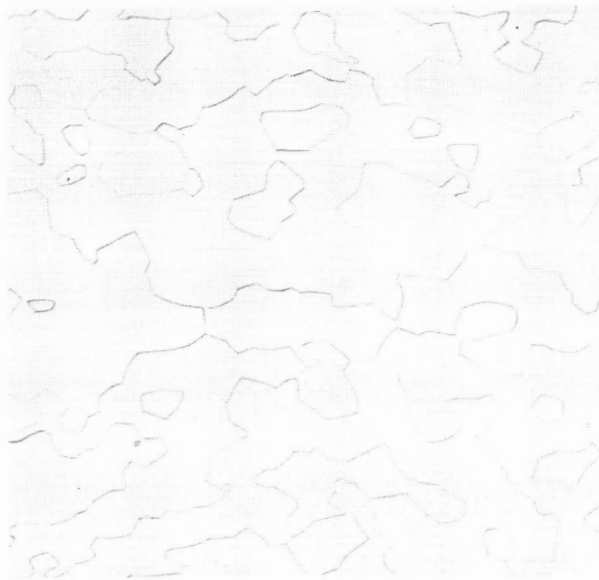
FIGURE 6 - Room Temperature Tensile Strength



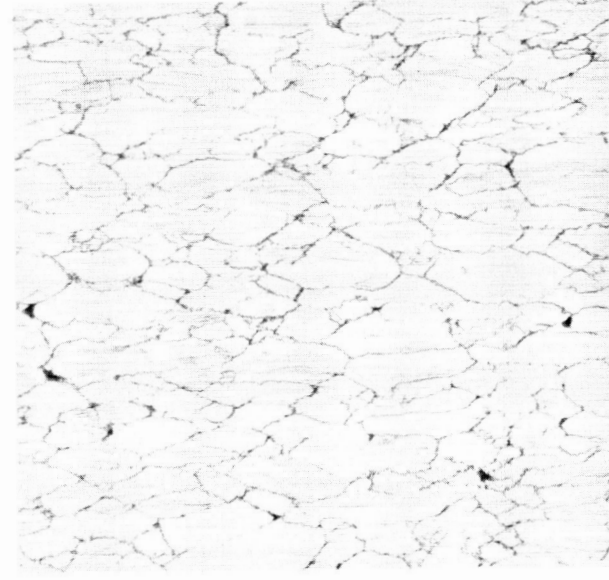
11,734 80X  
Weld Metal 2400°F Tensile Fracture



11,733 200X  
Base Metal 2400°F Tensile Fracture



8,680 200X  
Untested Base Metal  
(As Recrystallized, °F)



11,733 200X  
Typical Base Metal After 2400°F Test

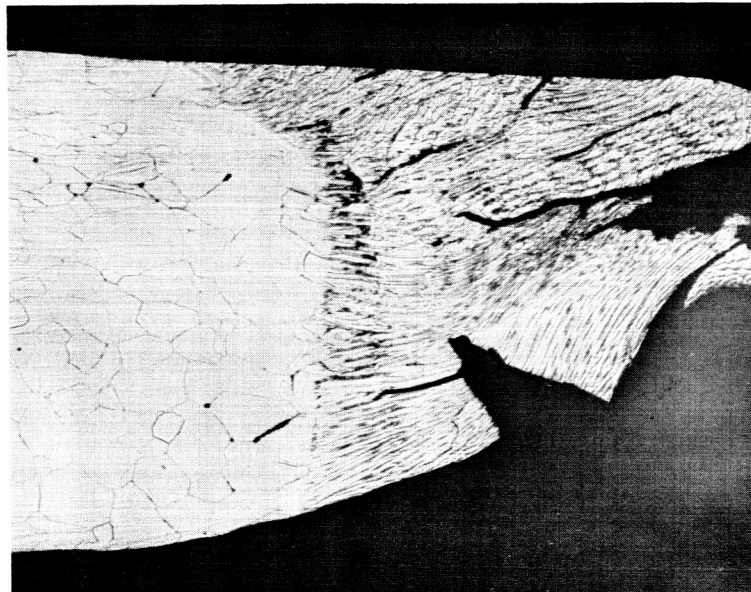
FIGURE 7 - Selected Metallography of Ta-10W Before and After Tensile Testing at 2400°F



10,218

Fracture Area from 2100°F Test

80X

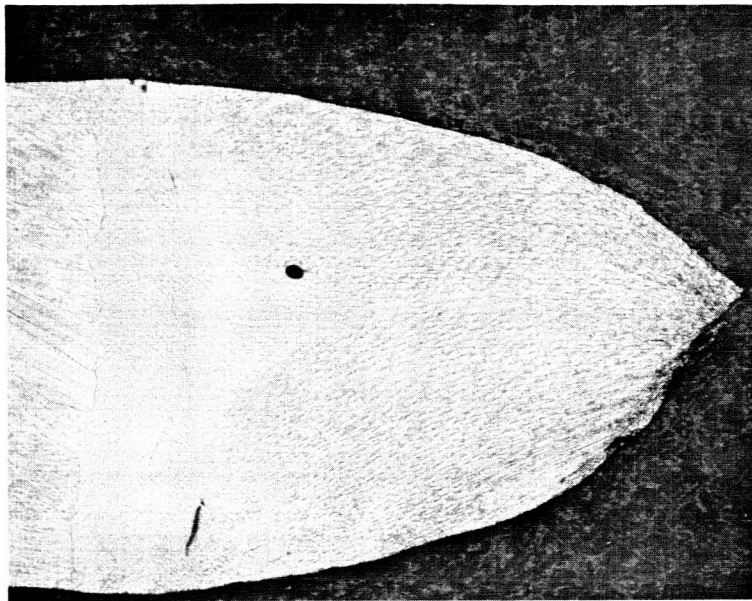


10,223

Fracture Area from 2400°F Test

100X

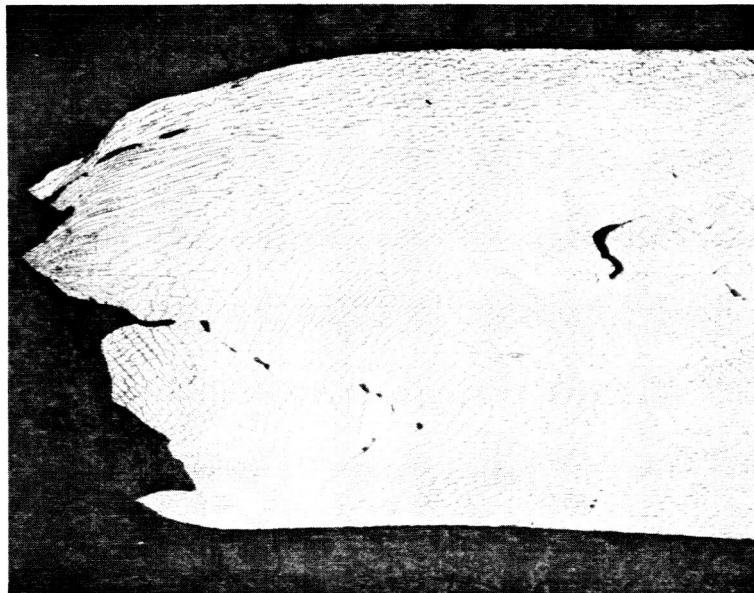
FIGURE 8 - T-111 Elevated Temperature Transverse Weld Tensile Fractures



10,224

Fracture Area from 2100°F Test

80X

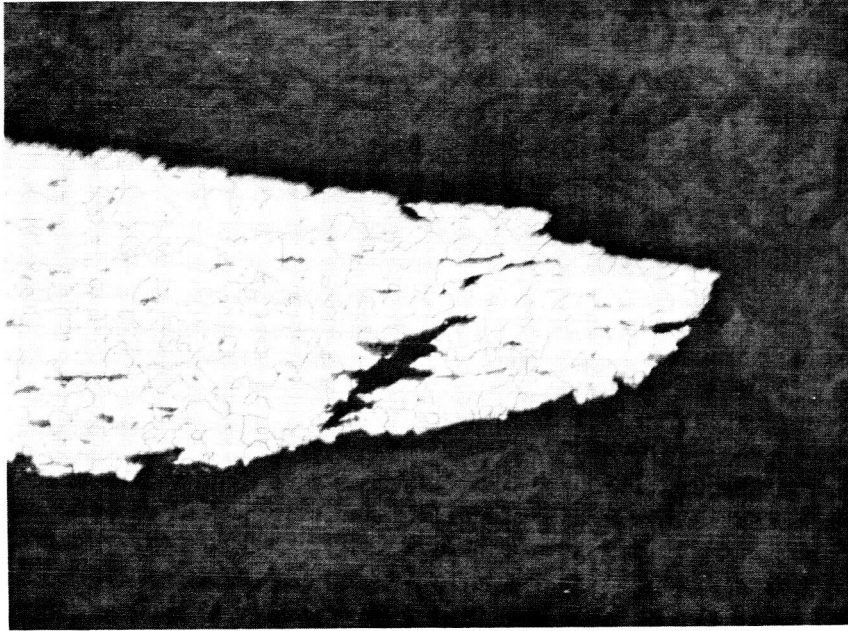


10,227

Fracture Area from 2400°F Test

80X

FIGURE 9 - T-222 Elevated Temperature Transverse Weld Tensile Fractures

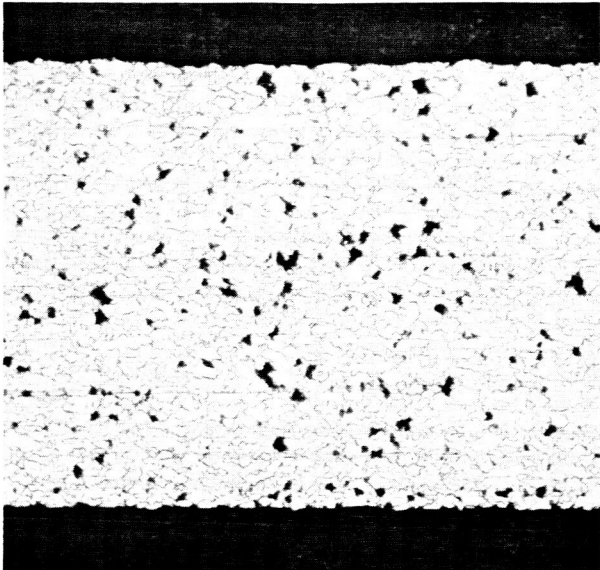


11,721

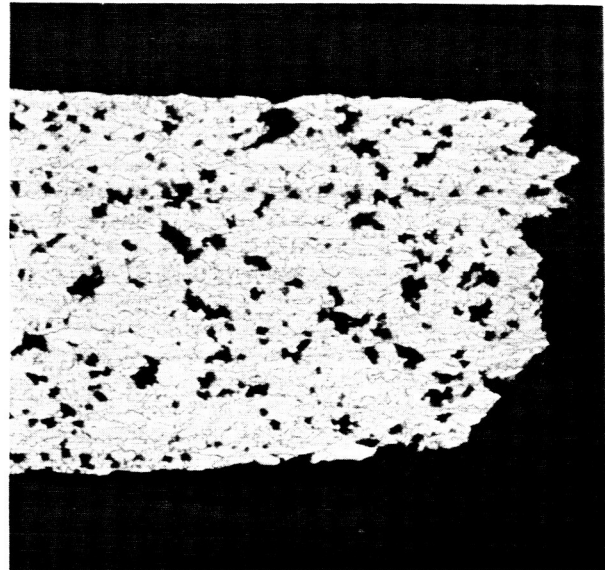
200X

FIGURE 10 - Base Metal Fracture of 2400°F B-66 Tensile Specimen

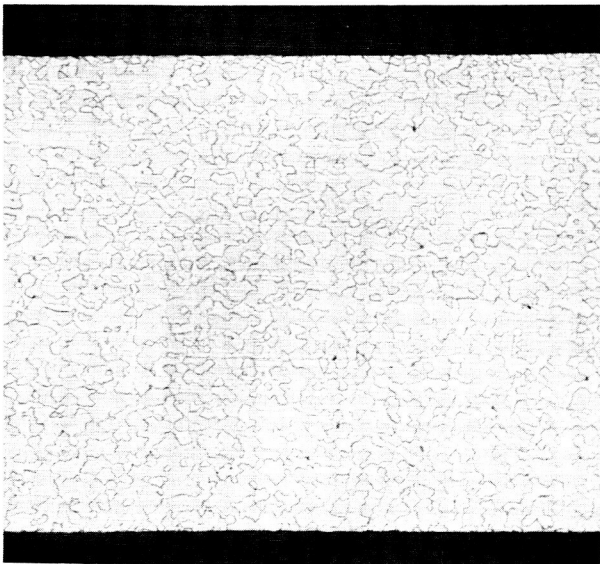




11,729B 100X  
Base Metal Specimen, General Area



11,729F 100X  
Base Metal, Fracture

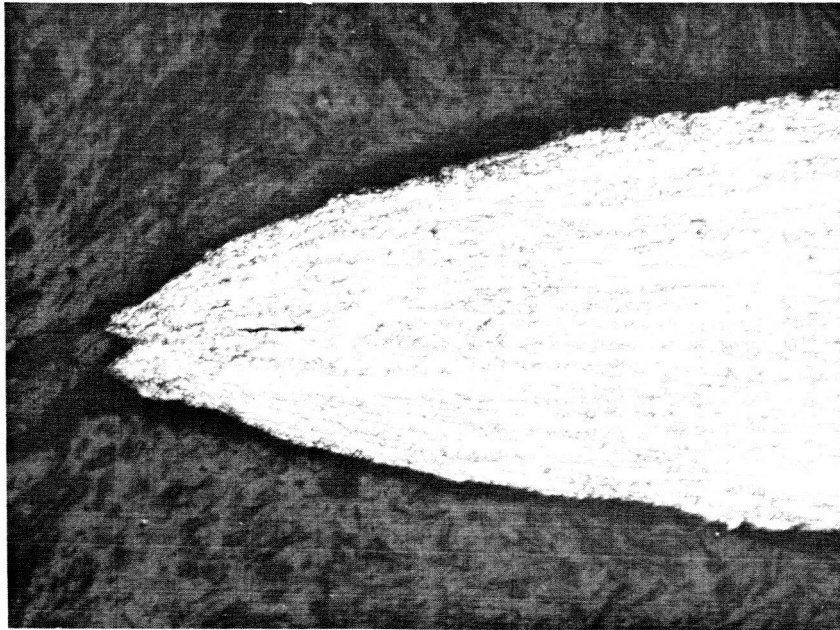


11,730B 80X  
Weld Specimen, General Base Metal Area



11,730F 80X  
Weld Specimen, Weld Fracture

FIGURE 11 - Microstructures of C-129Y Base Metal and Transverse  
Weld 2400°F Tensile Specimens



11,725

200X

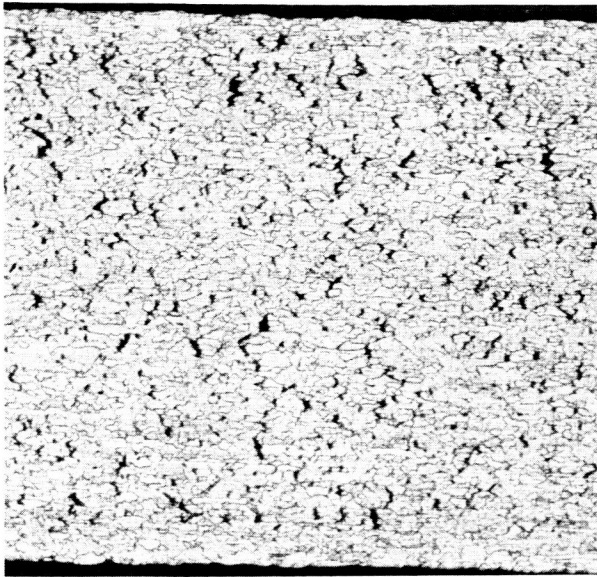
FIGURE 12 - Base Metal Fracture of the 2400°F Cb-752 Tensile Specimen



11,724

200X

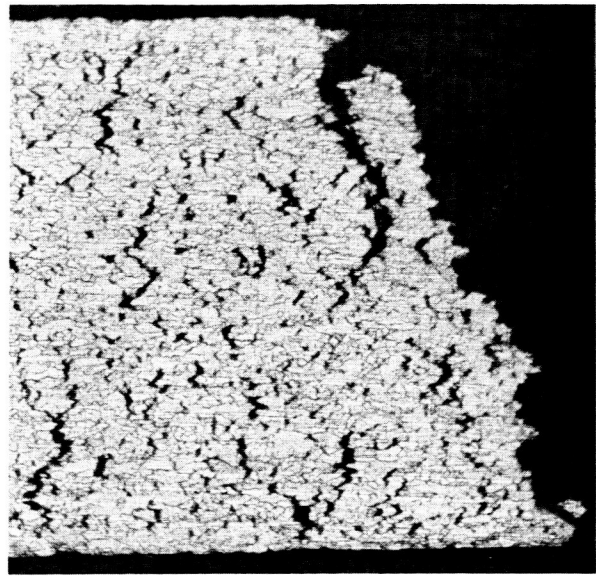
FIGURE 13 - Weld Fracture of the 2400°F Transverse D-43 Weld Tensile Specimen



11,731B

100X

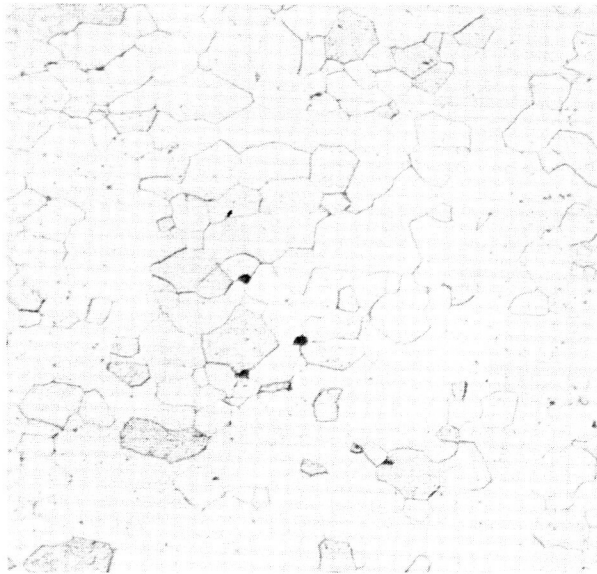
Base Metal, General Area



11,731F

100X

Base Metal, Fracture



11,732H

200X

Heat Affected Zone, General Area



11,732W

200X

Weld, General Area

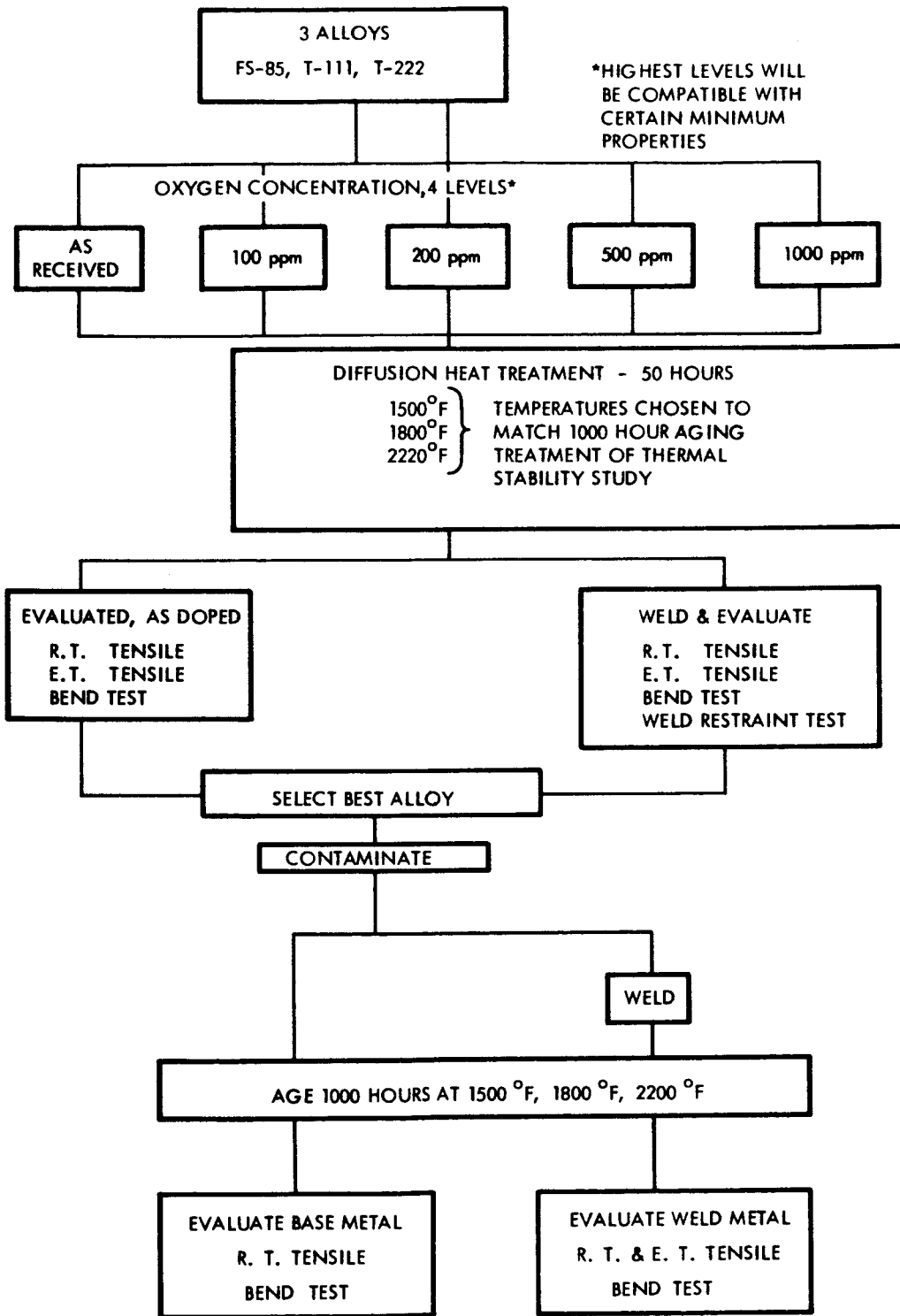
FIGURE 14 - Microstructure of D-43Y Tensile Specimen Tested at 2400°F



10,215

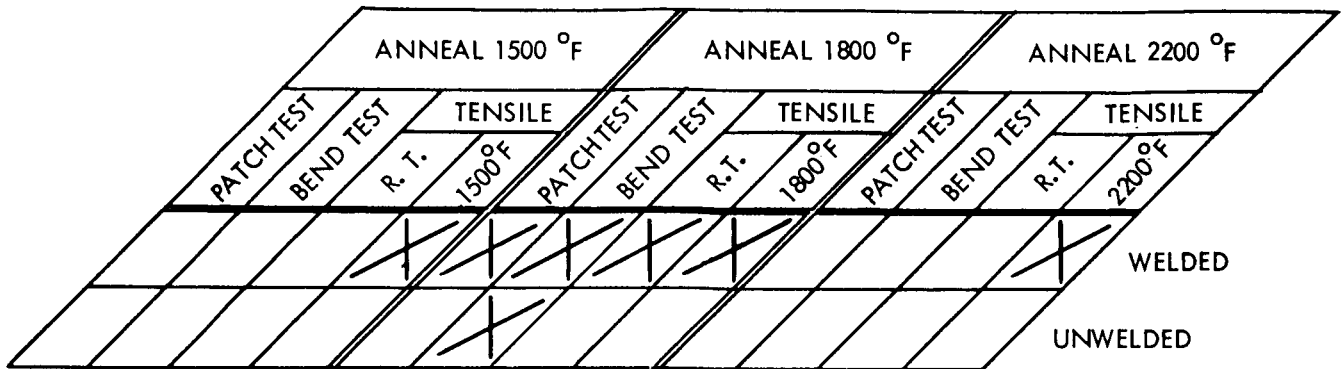
80X

FIGURE 15 - Weld Fracture of the 2400°F FS-85 Weld Tensile Specimen

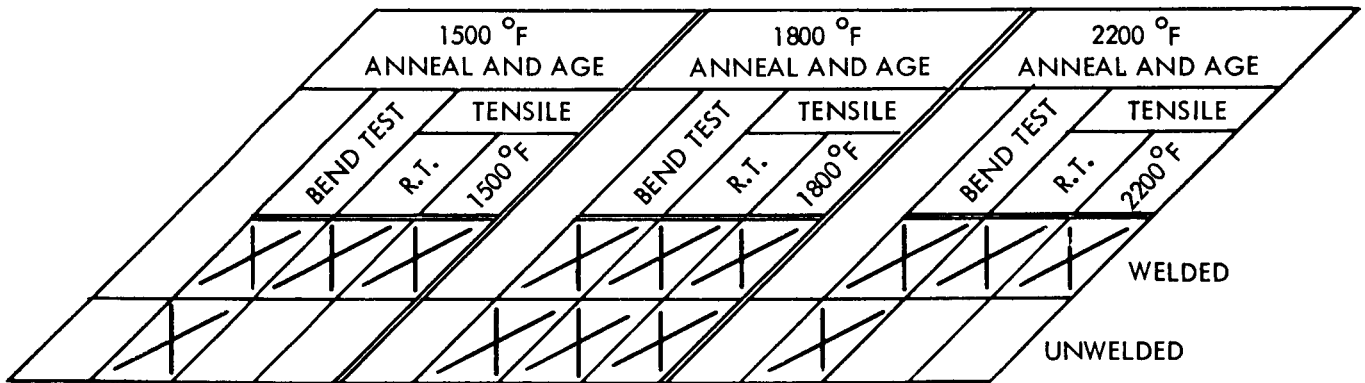


605807A

FIGURE 16 - Program Outline for Contaminated Alloy Weldability Evaluation



TASK I 3 ALLOYS X 5 OXYGEN LEVELS  
AS RECEIVED  
100 PPM  
200 PPM  
500 PPM  
1000 PPM



TASK II 1 ALLOY X 5 OXYGEN LEVELS  
AS RECEIVED  
100 PPM  
200 PPM  
500 PPM  
1000 PPM

610811-16A

FIGURE 17 - Detailed Outline of Specimen Requirements for Oxidation Program.

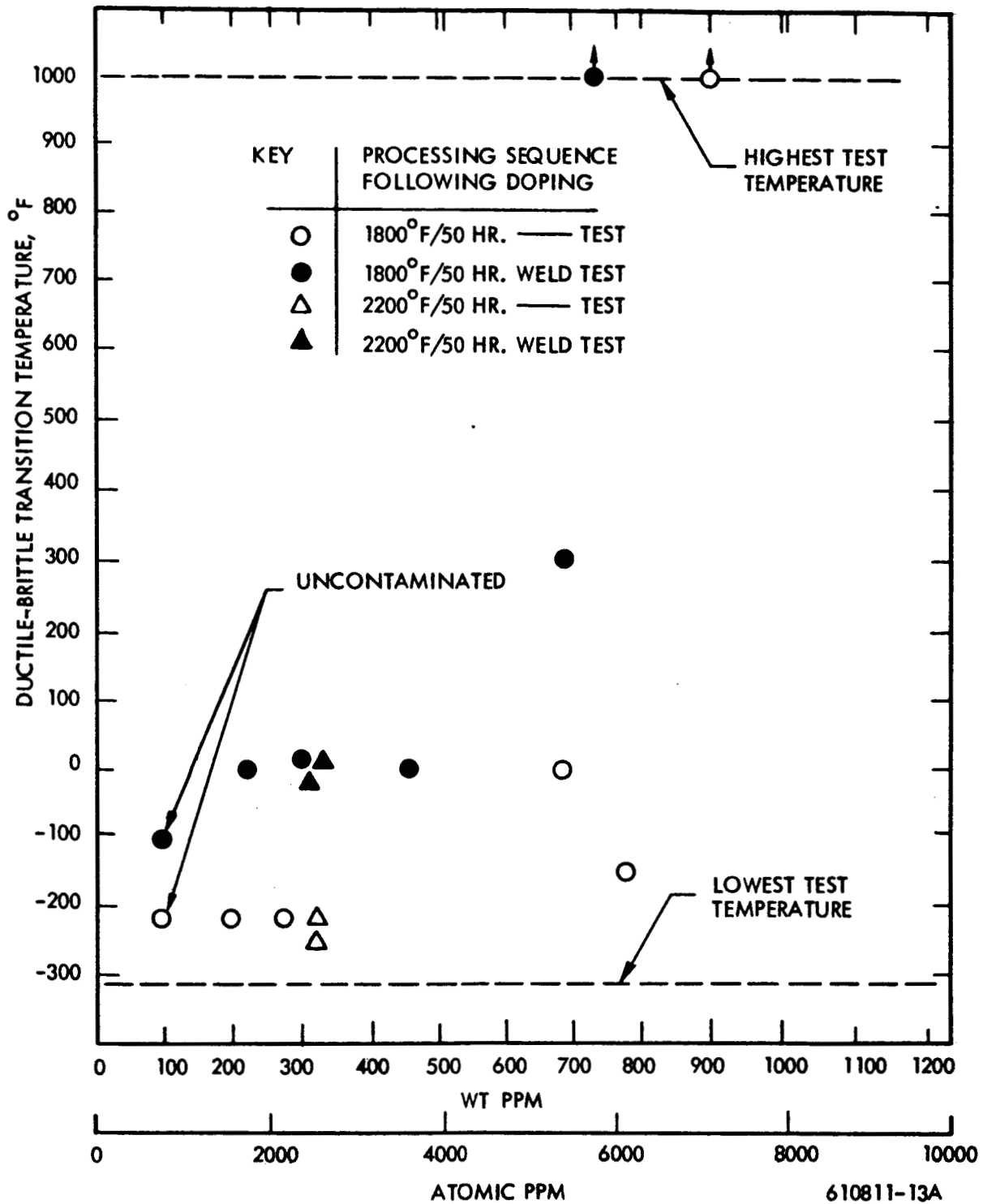


FIGURE 18 - FS-85, Variation of Ductile-Brittle Transition Temperature with Oxygen Content

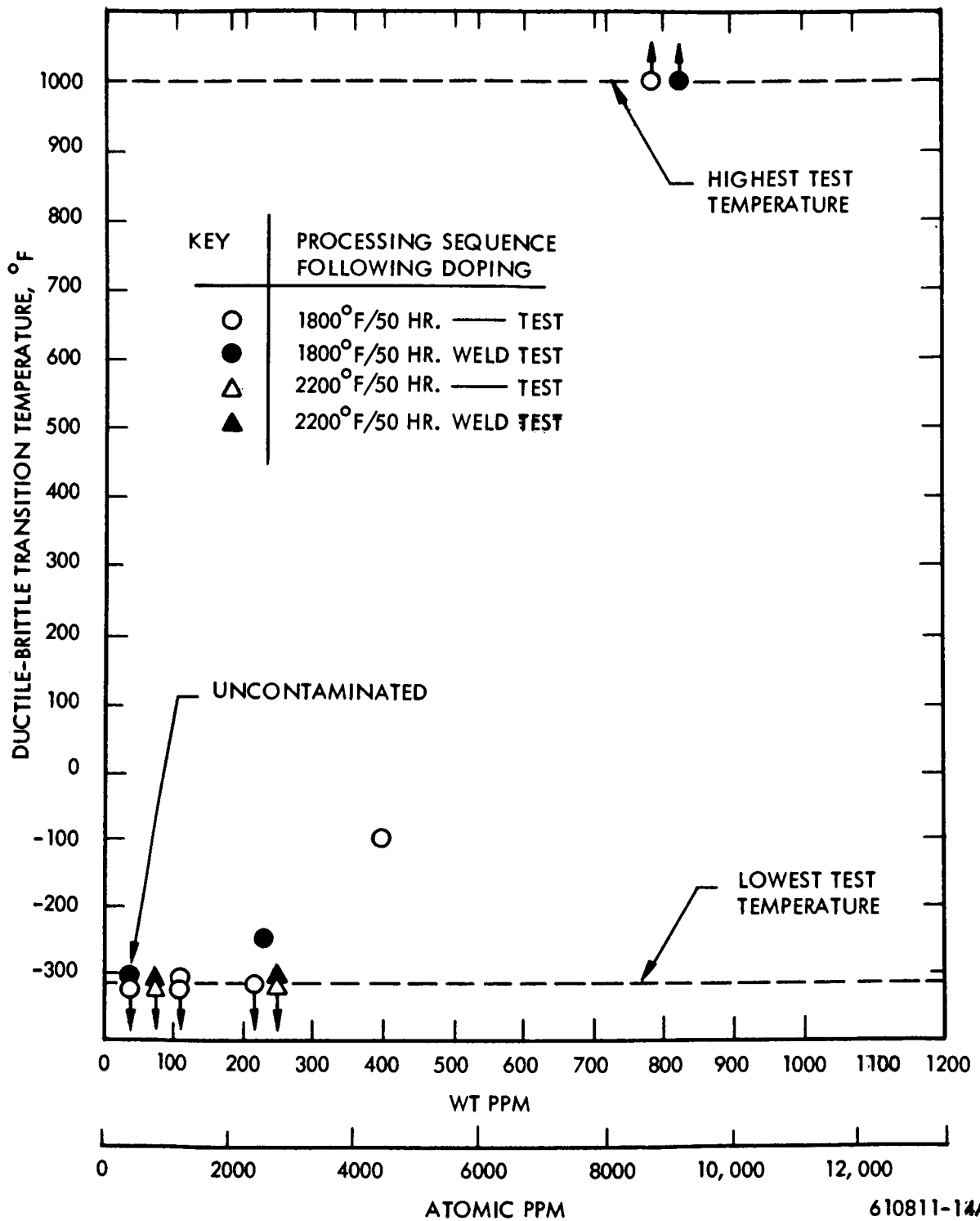
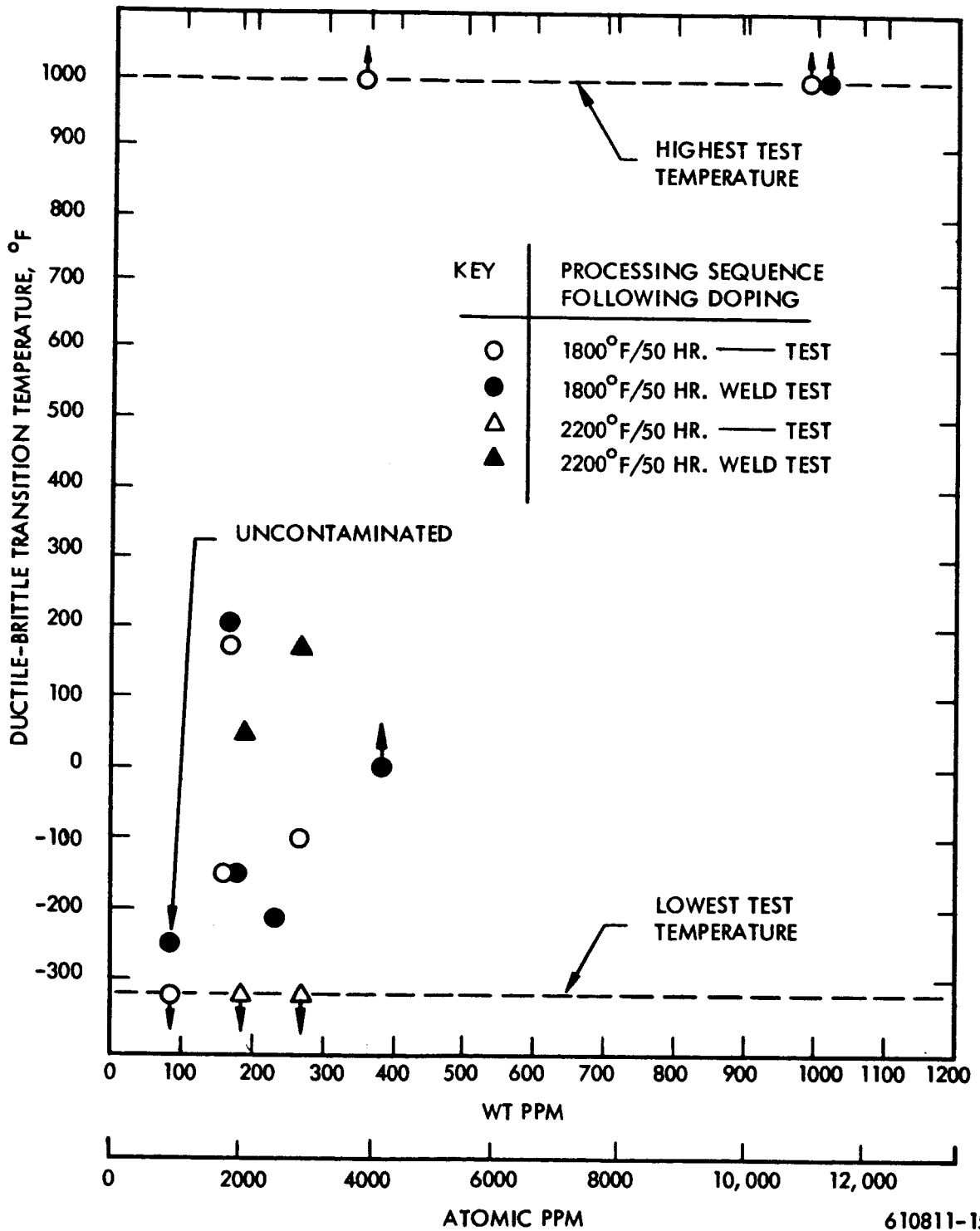


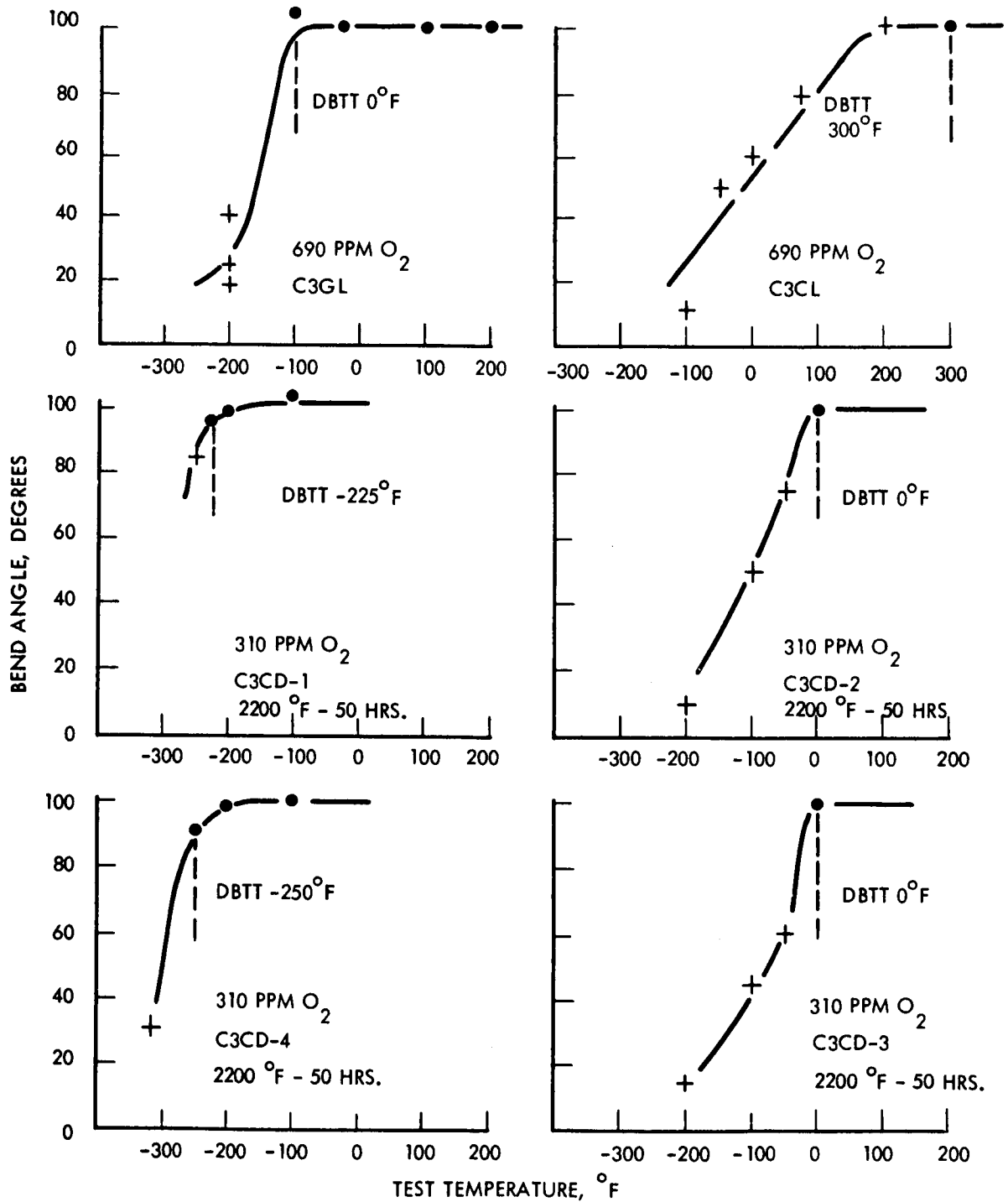
FIGURE 19 - T-111, Variation of Ductile-Brittle Transition Temperature with Oxygen Content





610811-15A

FIGURE 20 - T-222, Variation of Ductile-Brittle Transition Temperature with Oxygen Content

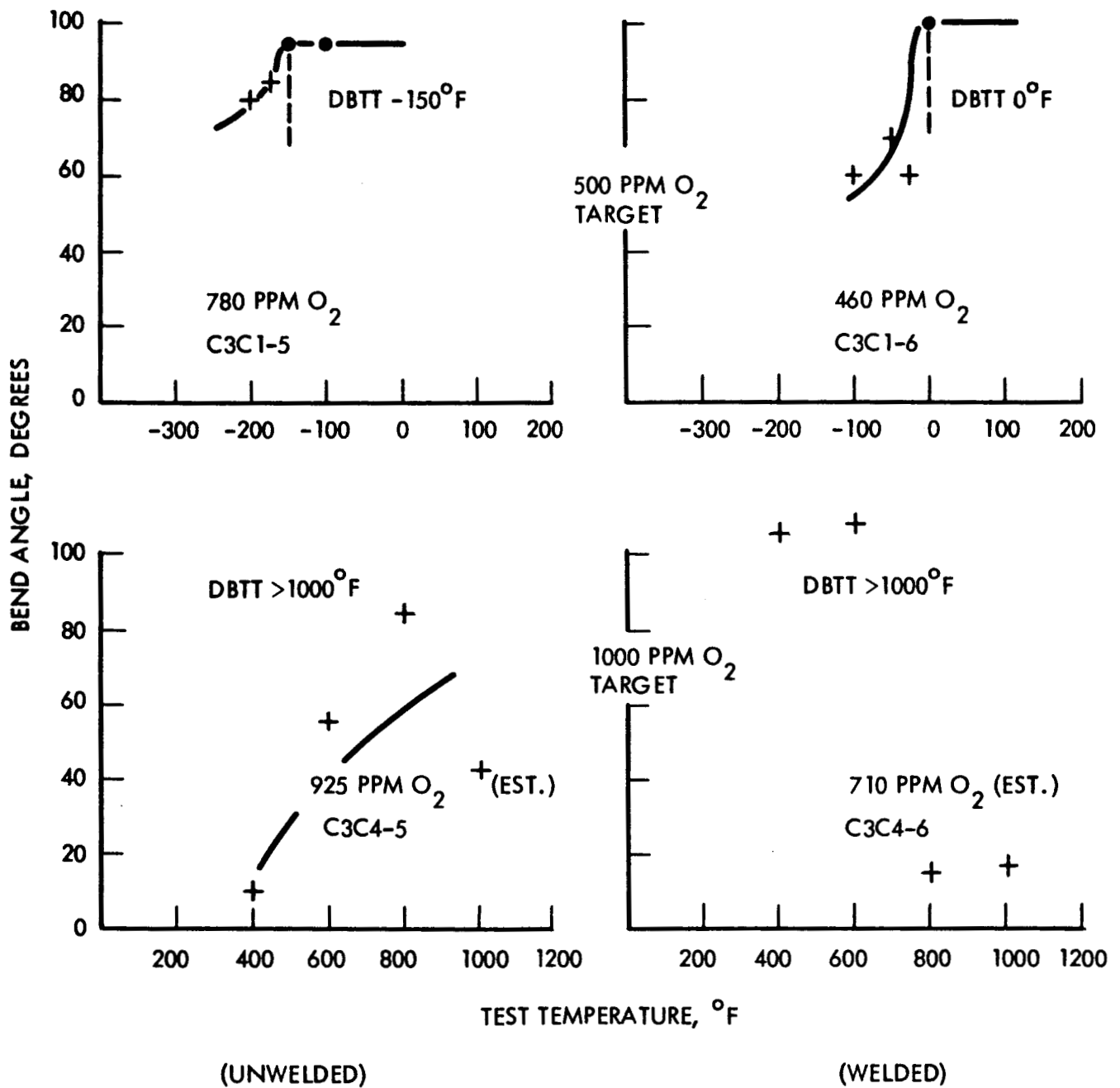


(UNWELDED)

(WELDED)

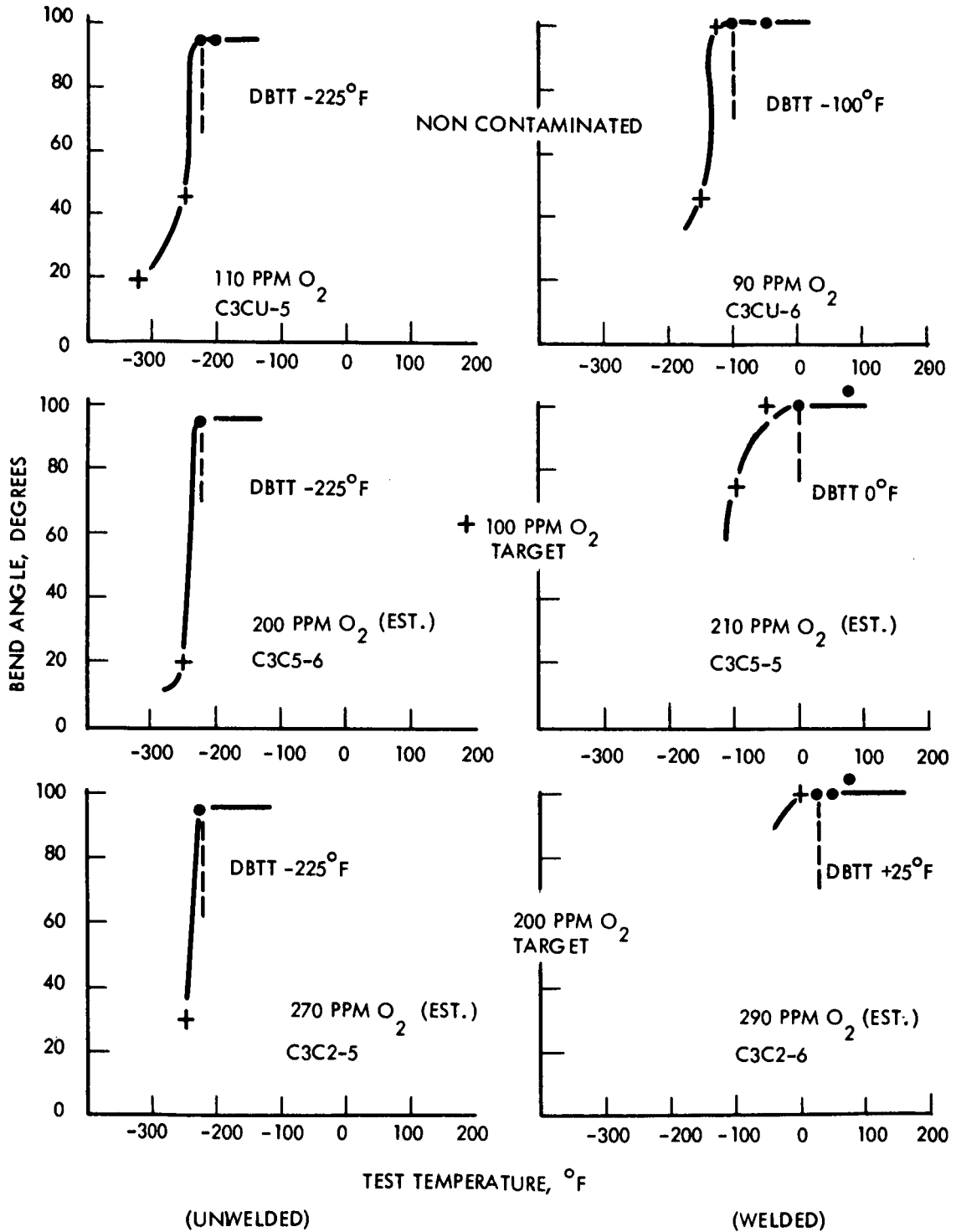
610811-4A

FIGURE 21 - Longitudinal Bend Test Results of FS-85, Low Level O<sub>2</sub> Content



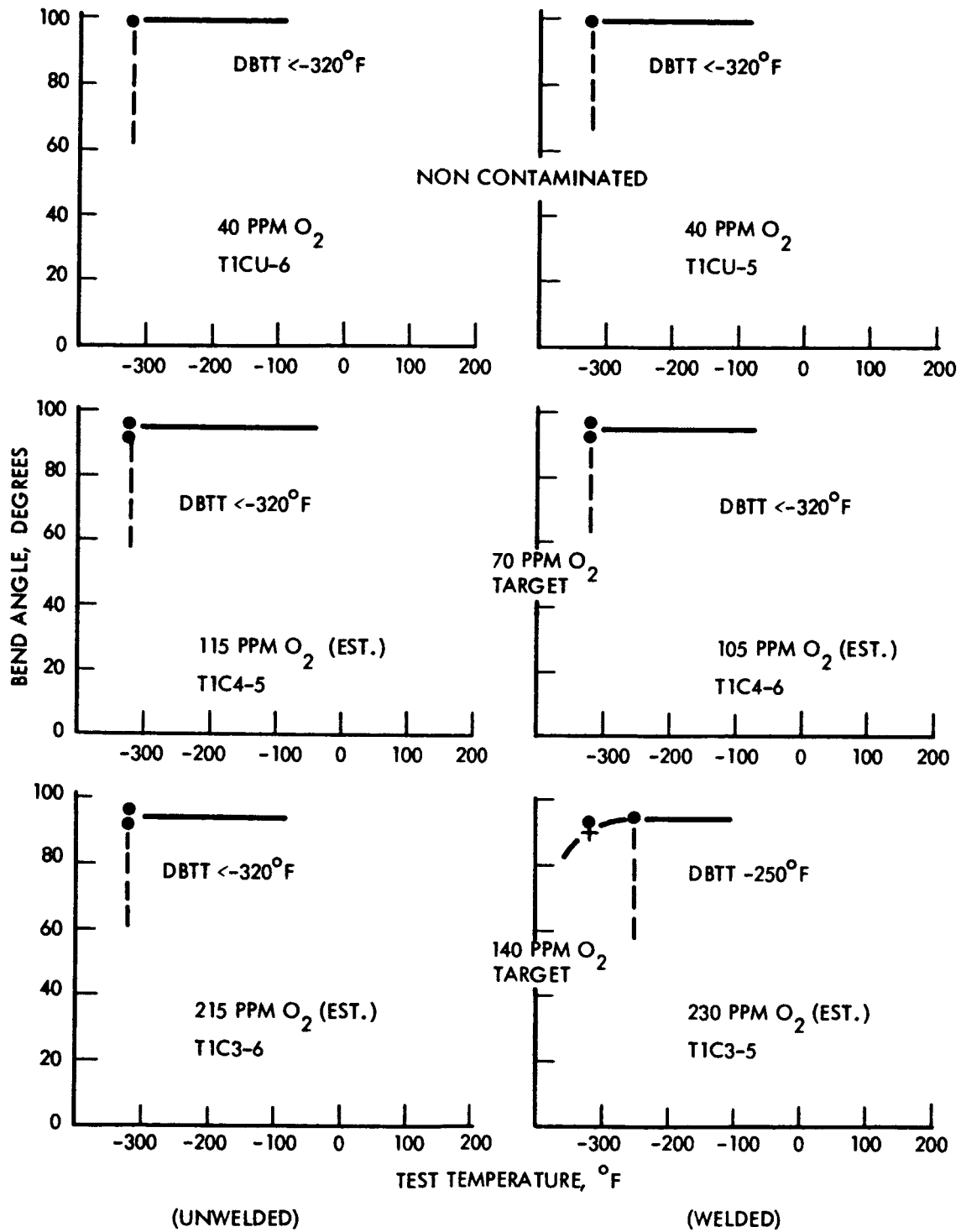
610811-2A

FIGURE 22 - Longitudinal Bend Test Results of FS-85, High Level O<sub>2</sub> Content



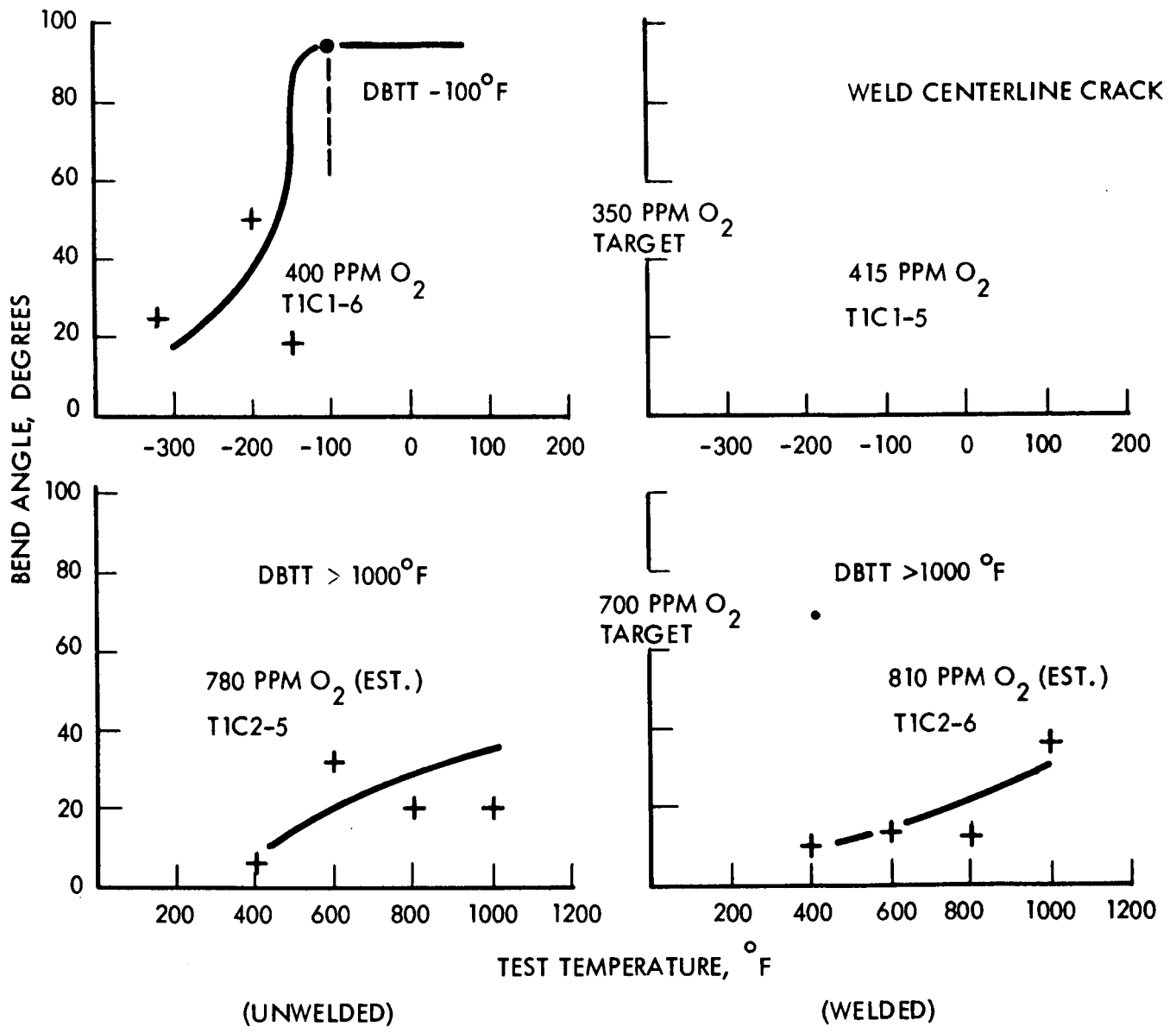
610811-3A

FIGURE 23 - Longitudinal Bend Test Results of FS-85, Preliminary Data



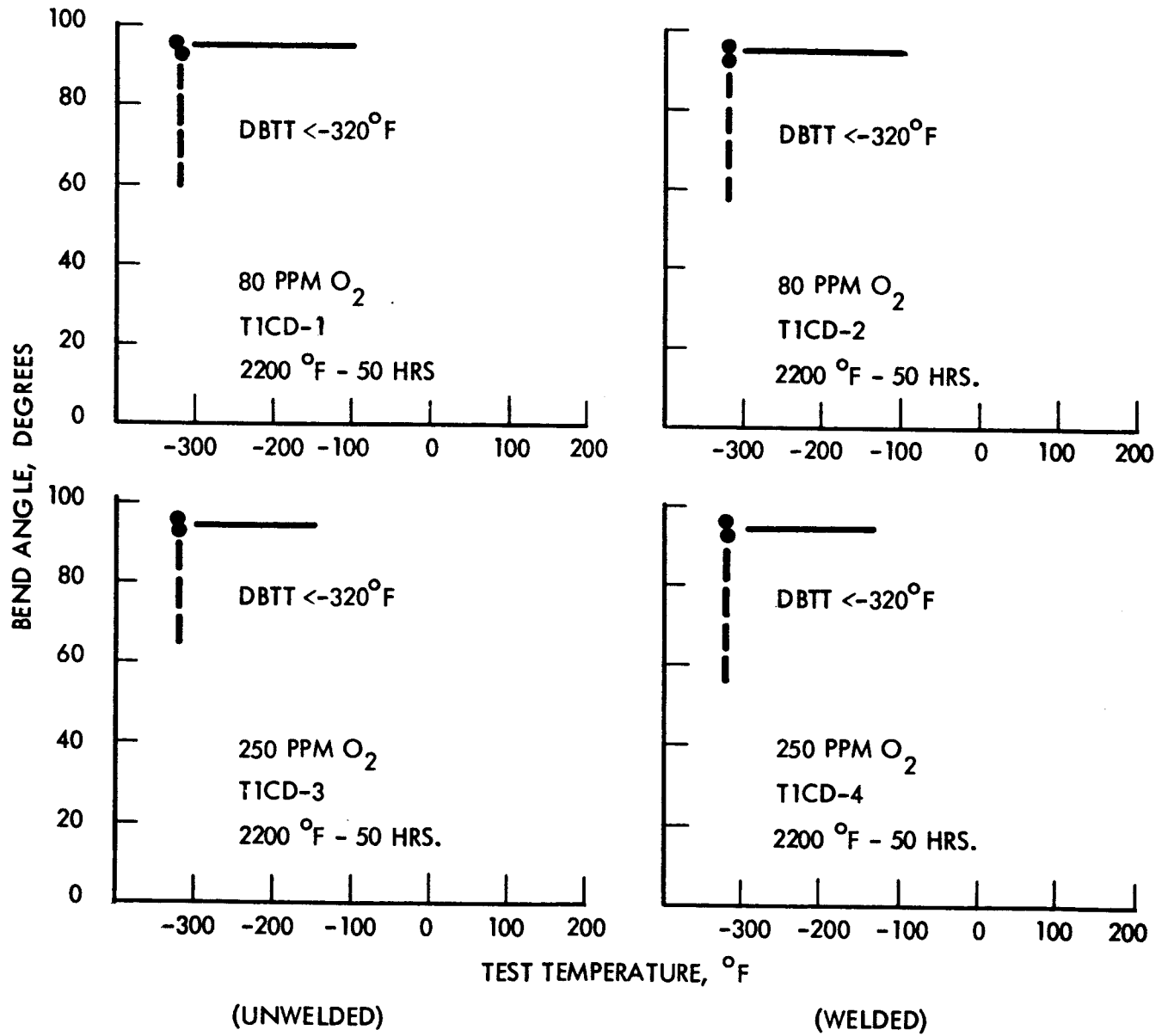
610811-5A

FIGURE 24 - Longitudinal Bend Test Results of T-111, Low Level O<sub>2</sub> Content



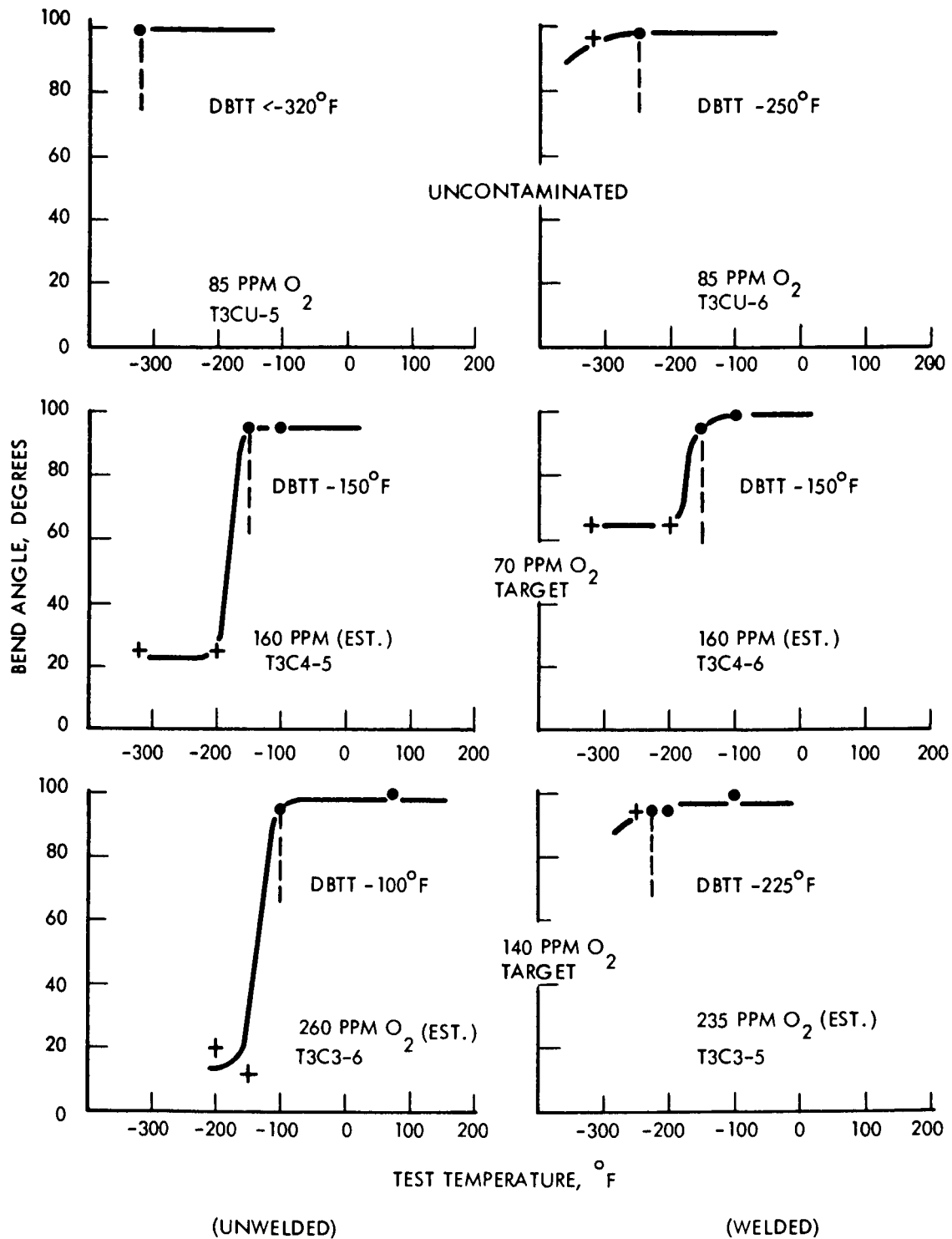
610811-6A

FIGURE 25 - Longitudinal Bend Test Results of T-111, High Level O<sub>2</sub> Content



610811-7A

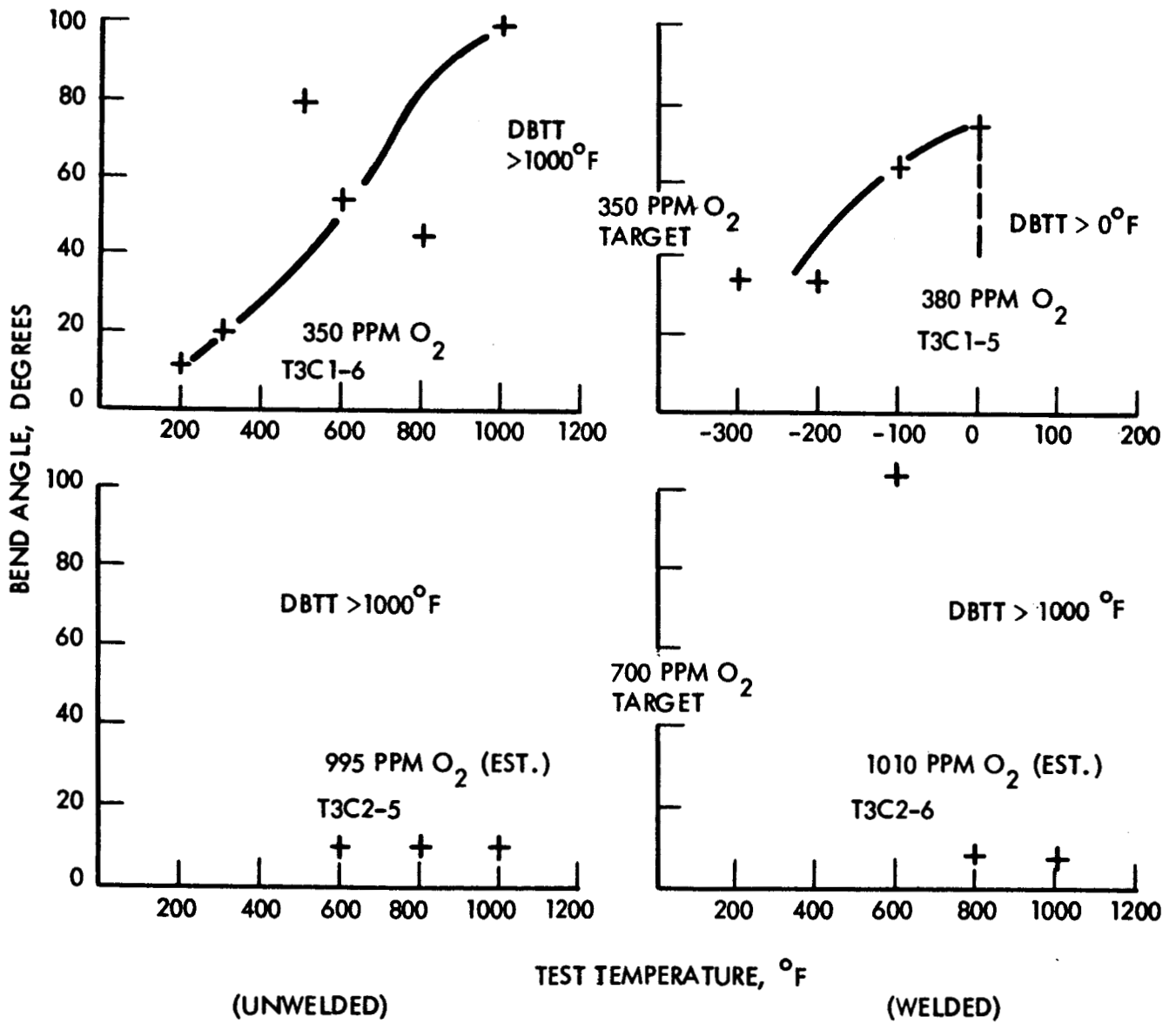
FIGURE 26 - Longitudinal Bend Test Results of T-111, Preliminary Data



610811-17A

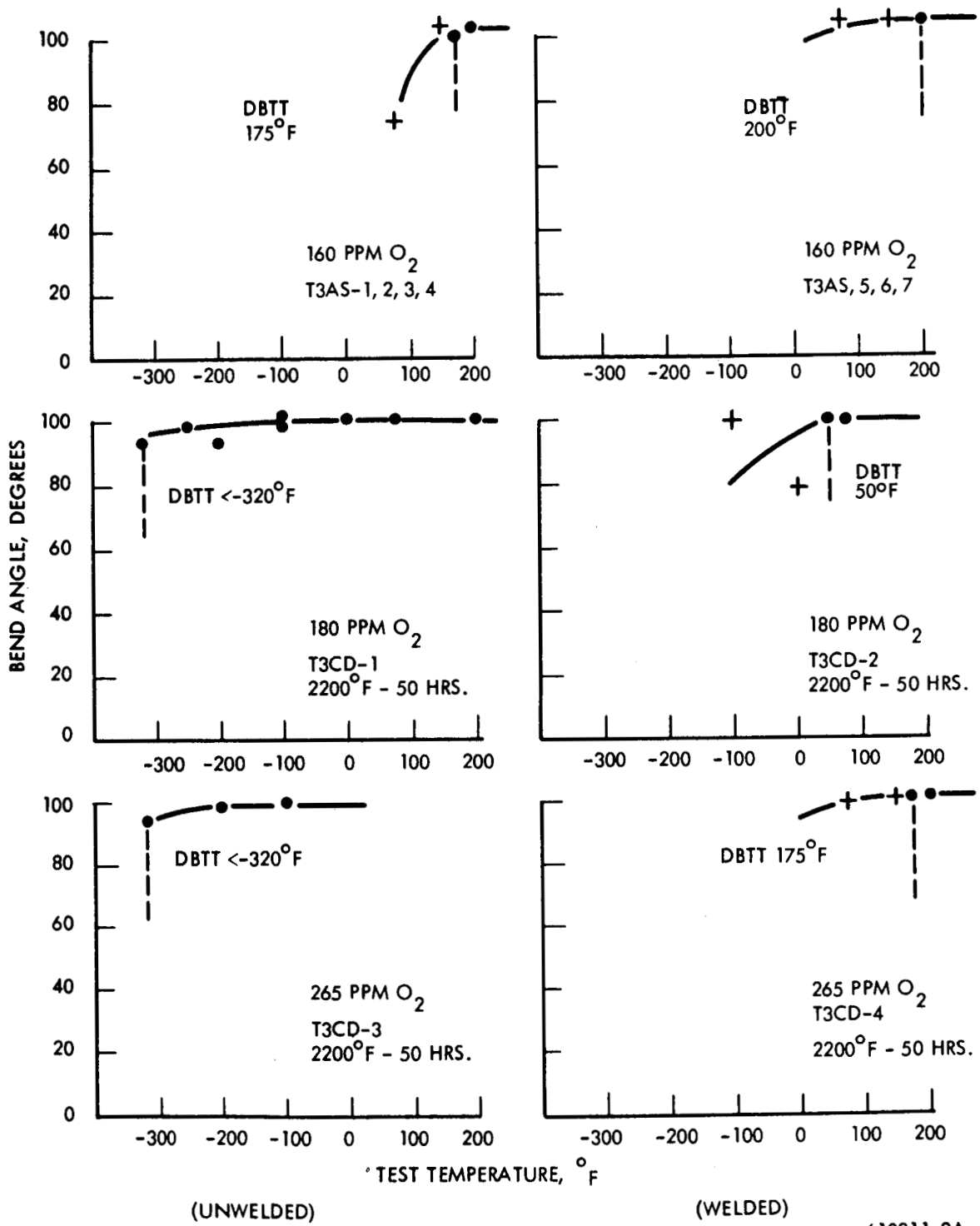
FIGURE 27 - Longitudinal Bend Test Results of T-222, Low Level O<sub>2</sub> Content





610811-9A

FIGURE 28 - Longitudinal Bend Test Results of T-222, High Level O<sub>2</sub> Content



610811-8A

FIGURE 29 - Longitudinal Bend Test Results of T-222, Preliminary Data

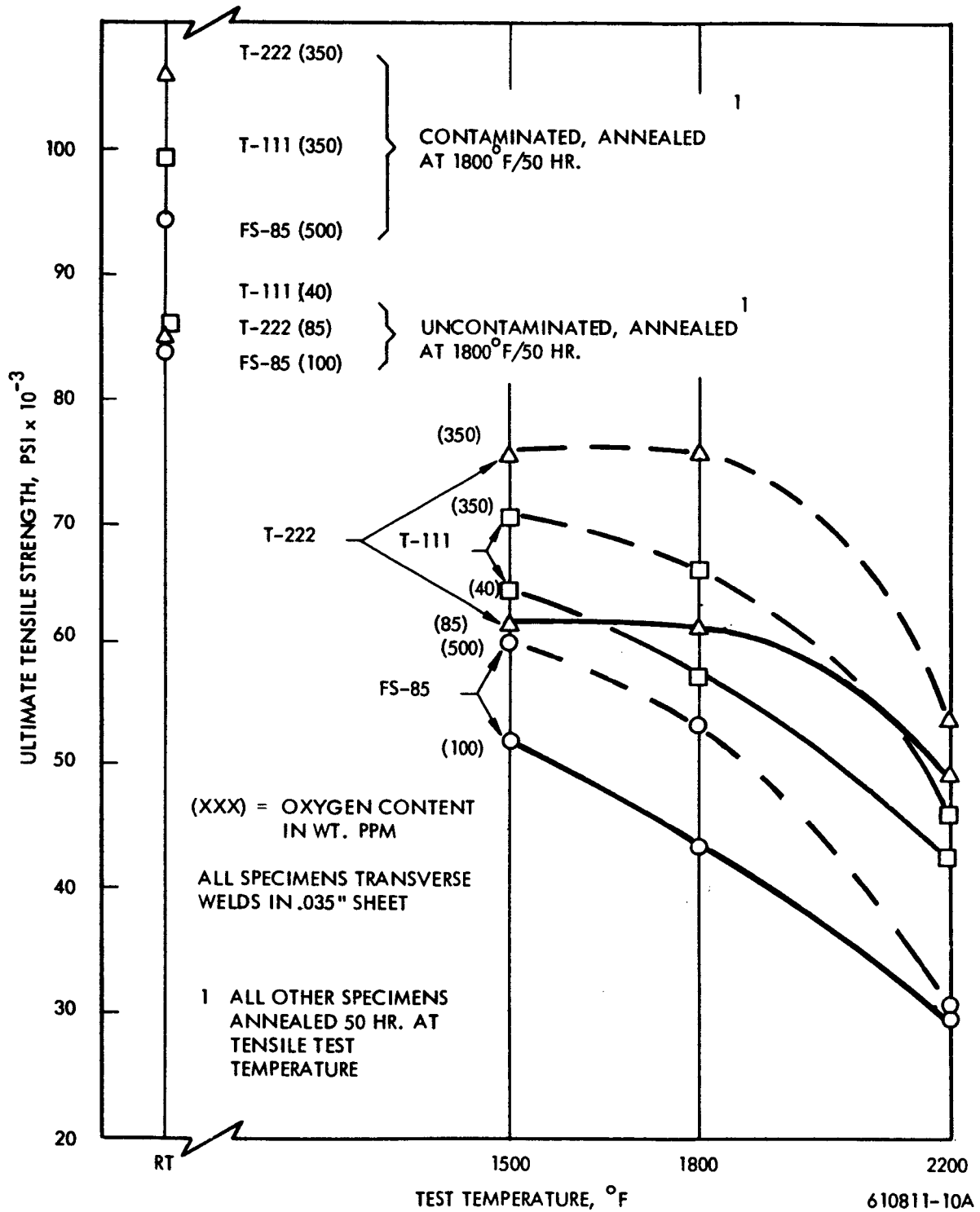


FIGURE 30 - Tensile Strength Versus Temperature at Two Oxygen Levels for FS-85, T-111, and T-222

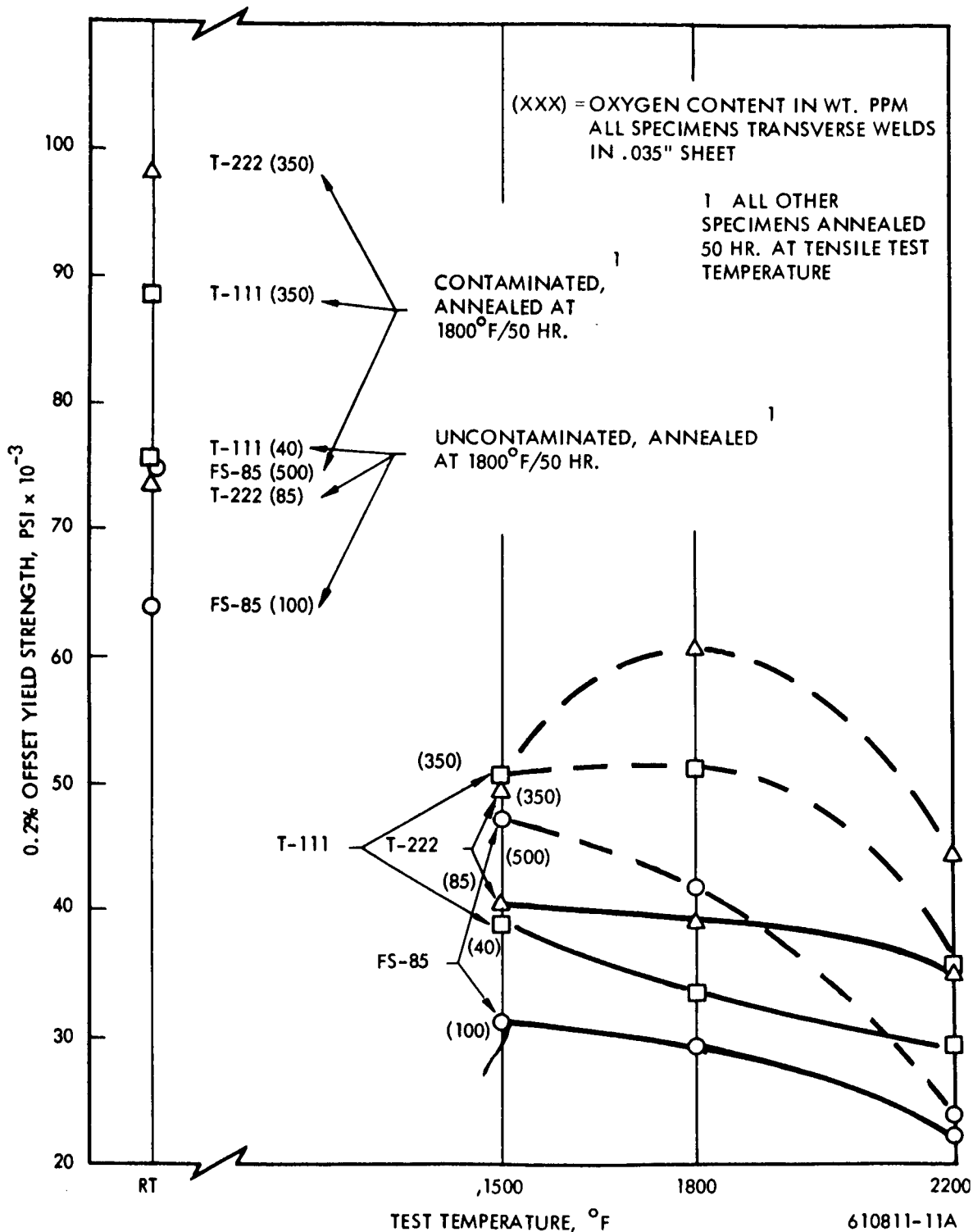


FIGURE 31 - Yield Strength Versus Temperature at Two Oxygen Levels for FS-85, T-111, and T-222

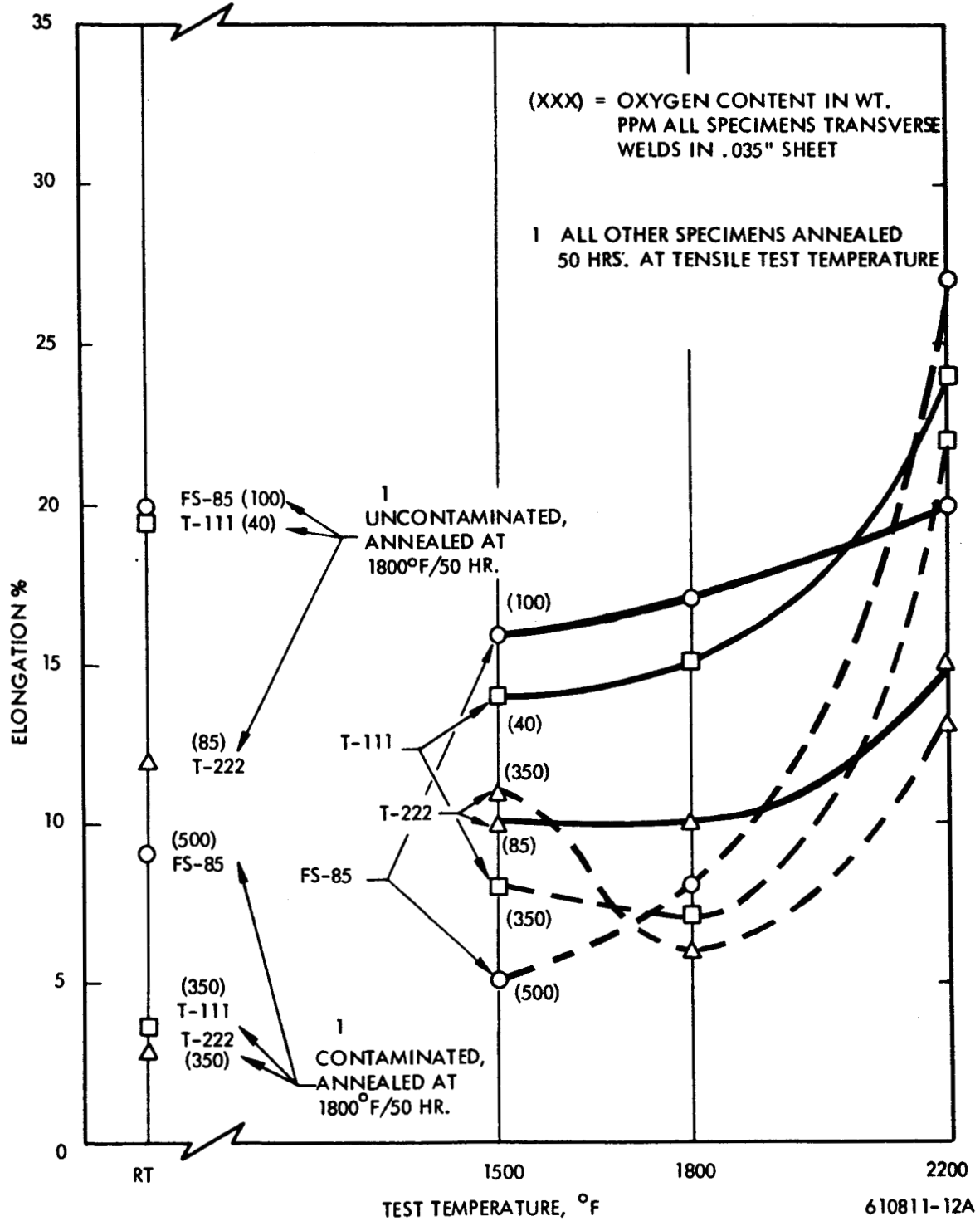


FIGURE 32 - Tensile Elongation Versus Temperature at Two Oxygen Levels for FS-85, T-111, and T-222

**DISTRIBUTION LIST**

TRW  
Caldwell Research Center  
23555 Euclid Avenue  
Cleveland, Ohio 44117  
Attn: Librarian  
Attn: G. J. Guarnieri

TRW  
New Devices Laboratories  
7209 Platt Avenue  
Cleveland, Ohio 44104  
Attn: Librarian

National Aeronautics and Space Adm.  
Washington, D. C. 20546  
Attn: Walter C. Scott  
Attn: James J. Lynch (RN)  
Attn: George C. Deutsch (RR)

National Aeronautics and Space Adm.  
Scientific and Technical Inf. Facility  
Box 5700  
Bethesda, Maryland 21811

National Aeronautics and Space Adm.  
Ames Research Center  
Moffet Field, California 94035  
Attn: Librarian

National Aeronautics and Space Adm.  
Goddard Space Flight Center  
Greenbelt, Maryland 20771  
Attn: Librarian

National Aeronautics and Space Adm.  
Langley Research Center  
Hampton, Virginia 23365  
Attn: Librarian

National Aeronautics and Space Adm.  
Manned Spacecraft Center  
Houston, Texas 77001  
Attn: Librarian

National Aeronautics and Space Adm.  
George C. Marshall Space Flight Center  
Huntsville, Alabama 35812  
Attn: Librarian  
Attn: Wm. A. Wilson

National Aeronautics and Space Adm.  
Jet Propulsion Laboratory  
4800 Oak Grove Drive  
Pasadena, California 91103  
Attn: Librarian

National Aeronautics and Space Adm.  
21000 Brookpark Road  
Cleveland, Ohio 44135  
Attn: Librarian  
Attn: Dr. Bernard Lubarsky  
Attn: Mr. Roger Mather  
Attn: Mr. G. M. Ault  
Attn: Mr. J. Joyce  
Attn: Mr. P. E. Moorhead  
Attn: Mr. N. T. Musial  
Attn: Mr. T. Strom  
Attn: Mr. T. A. Moss  
Attn: Dr. Louis Rosenblum  
Attn: J. Creagh  
Attn: Mr. J. Dilley  
Attn: Mr. G. K. Watson  
Attn: Mr. T. Moore  
Attn: Mr. G. Tulsiaik  
Attn: NASA-Lewis Laboratory Report Central  
Section

National Aeronautics and Space Adm.  
Western Operations Office  
150 Pico Boulevard  
Santa Monica, California 90406  
Attn: Mr. John Keeler

National Bureau of Standards  
Washington 25, D. C.  
Attn: Librarian



Astronuclear  
Laboratory

Aeronautical Systems Division  
Wright-Patterson Air Force Base, Ohio  
Attn: Charles Ambruster  
Attn: T. Cooper  
Attn: Librarian  
Attn: John L. Morris  
Attn: H. J. Middendorp

Army Ordnance Frankford Arsenal  
Bridesburg Station  
Philadelphia 37, Pennsylvania  
Attn: Librarian

Bureau of Ships  
Dept. of the Navy  
Washington 25, D. C.  
Attn: Librarian

Bureau of Weapons  
Research and Engineering  
Material Division  
Washington 25, D. C.  
Attn: Librarian

U. S. Atomic Energy Commission  
Technical Reports Library  
Washington 25, D. C.  
Attn: J. M. O'Leary

U. S. Atomic Energy Commission  
Germantown, Maryland  
Attn: Col. E. L. Douthett  
Attn: H. Rothen  
Attn: Major Gordon Dicker

U. S. Atomic Energy Commission  
Technical Information Service Extension  
P. O. Box 62  
Oak Ridge, Tennessee

U. S. Atomic Energy Commission  
Washington 25, C. C.  
Attn: M. J. Whitman

Argonne National Laboratory  
9700 South Cross Avenue  
Argonne, Illinois  
Attn: Librarian

Brookhaven National Laboratory  
Upton, Long Island, New York  
Attn: Librarian

Oak Ridge National Laboratory  
Oak Ridge, Tennessee  
Attn: W. O. Harms  
Attn: Dr. A. J. Miller  
Attn: Librarian  
Attn: N. T. Bray

Office of Naval Research  
Power Division  
Washington 25, D. C.  
Attn: Librarian

U. S. Naval Research Laboratory  
Washington 25, D. C.  
Attn: Librarian

Advanced Technology Laboratories  
Division of American Standard  
369 Whisman Road  
Mountain View, California  
Attn: Librarian

Aerojet General Corporation  
P. O. Box 296  
Azusa, California  
Attn: Librarian

Aerojet General Nucleonics  
P. O. Box 77  
San Ramon, California  
Attn: Librarian

AiResearch Manufacturing Company  
Sky Harbor Airport  
402 South 36th Street  
Phoenix, Arizona  
Attn: Librarian  
Attn: E. A. Kovacevich

**AiResearch Manufacturing Company**  
9851-9951 Sepulveda Boulevard  
Los Angeles 45, California  
Attn: Librarian

**I. I. T. Research Institute**  
10 W. 35th Street  
Chicago, Illinois 60616

**Atomics International**  
8900 DeSoto Avenue  
Canoga Park, California

**Avco**  
Research and Advanced Development Dept.  
201 Lowell Street  
Wilmington, Massachusetts  
Attn: Librarian

**Babcock and Wilcox Company**  
Research Center  
Alliance, Ohio  
Attn: Librarian

**Battelle Memorial Institute**  
505 King Avenue  
Columbus, Ohio  
Attn: C. M. Allen  
Attn: Librarian  
Attn: Defense Metals Inf. Center

**The Bendix Corporation**  
Research Laboratories Div.  
Southfield, Detroit 1, Michigan  
Attn: Librarian

**Bell Aerosystems Co.**  
P. O. Box 1  
Buffalo 5, New York  
Attn: E. J. King

**The Boeing Company**  
Seattle, Washington  
Attn: Librarian

**Brush Beryllium Company**  
17876 St. Clair Avenue  
Cleveland, Ohio 44110  
Attn: Librarian

**Carborundum Company**  
Niagara Falls, New York  
Attn: Librarian

**Chance Vought Aircraft Inc.**  
P. O. Box 5907  
Dallas 22, Texas  
Attn: Librarian

**Clevite Corporation**  
Mechanical Research Division  
540 East 105th Street  
Cleveland 8, Ohio  
Attn: Mr. N. C. Beerli

**Climax Molybdenum Company of Michigan**  
1600 Huron Parkway  
Ann Arbor, Michigan  
Attn: Librarian

**Convair Astronautics**  
50001 Kerry Villa Road  
San Diego 11, California  
Attn: Librarian

**E. I. duPont deNemours and Co., Inc.**  
Wilmington 98, Delaware  
Attn: Librarian

**Electro-Optical Systems, Inc.**  
Advanced Power Systems Division  
Pasadena, California  
Attn: Librarian

**Fansteel Metallurgical, Corp.**  
North Chicago, Illinois  
Attn: Librarian





Astronuclear  
Laboratory

Ford Motor Company  
Aeronutronics  
Newport Beach, California  
Attn: Librarian

General Dynamics/General Atomic  
P. O. Box 608  
San Diego, California 92112  
Attn: Librarian

General Electric Company  
Atomic Power Equipment Div.  
P. O. Box 1131  
San Jose, California

General Electric Company  
Flight Propulsion Laboratory Dept.  
Cincinnati 15, Ohio  
Attn: Librarian  
Attn: Dr. J.W. Semmel

General Electric Company  
Missile and Space Vehicle Dept.  
3198 Chestnut Street  
Philadelphia 4, Pennsylvania  
Attn: Librarian

General Electric Company  
Vallecitos  
Vallecitos Atomic Lab.  
Pleasanton, California  
Attn: Librarian

Herring Corp.  
7356 Greenback Drive  
Hollywood, California 91605  
Attn: Don Adams

General Dynamics/Fort Worth  
P. O. Box 748  
Fort Worth, Texas  
Attn: Librarian

General Motors Corporation  
Allison Division  
Indianapolis 6, Indiana  
Attn: Librarian

Hamilton Standard  
Div. of United Aircraft Corp.  
Windsor Locks, Connecticut  
Attn: Librarian

Hughes Aircraft Company  
Engineering Division  
Culver City, California  
Attn: Librarian

Lockheed Missiles and Space Div.  
Lockheed Aircraft Corp.  
Sunnyvale, California  
Attn: Librarian

Marquardt Aircraft Co.  
P. O. Box 2013  
Van Nuys, California  
Attn: Librarian

The Martin Company  
Baltimore 3, Maryland  
Attn: Librarian

The Martin Company  
Nuclear Division  
P. O. Box 5042  
Baltimore 20, Maryland  
Attn: Librarian

Martin Marietta Corp.  
Metals Technology Laboratory  
Wheeling, Illinois

Massachusetts Institute of Technology  
Cambridge 39, Massachusetts  
Attn: Librarian

Materials Research and Development  
Manlabs Inc.  
21 Erie Street  
Cambridge 39, Massachusetts

Materials Research Corporation  
Orangeburg, New York  
Attn: Librarian

McDonnell Aircraft  
St. Louis, Missouri  
Attn: Librarian

MSA Research Corporation  
Callery, Pennsylvania  
Attn: Librarian

North American Aviation  
Los Angeles Division  
Los Angeles 9, California  
Attn: Librarian

National Research Corp.  
Metals Division  
45 Industrial Place  
Newton, Massachusetts 02164  
Attn: Dr. M. L. Torte  
Director of Metallurgical Research

Lawrence Radiation Laboratory  
Livermore, California  
Attn: Dr. James Hadley  
Head, Reactor Division

Pratt & Whitney Aircraft  
400 Main Street  
East Hartford 8, Connecticut  
Attn: Librarian

Republic Aviation Corporation  
Farmingdale, Long Island, New York  
Attn: Librarian

Solar  
2200 Pacific Highway  
San Diego 12, California

Southwest Research Institute  
8500 Culebra Road  
San Antonio 6, Texas  
Attn: Librarian

Rocketdyne  
Canoga Park, California  
Attn: Librarian

Superior Tube Co.  
Norristown, Pennsylvania  
Attn: Mr. A. Bound

Sylvania Electric Products, Inc.  
Chem. & Metallurgical  
Towanda, Pennsylvania  
Attn: Librarian

Temescal Metallurgical  
Berkeley, California  
Attn: Librarian

Union Carbide Stellite Corp.  
Kokomo, Indiana  
Attn: Librarian

Union Carbide Metals  
Niagara Falls, New York  
Attn: Librarian

Union Carbide Nuclear Company  
P. O. Box X  
Oak Ridge, Tennessee  
Attn: X-10 Laboratory Records Department

United Nuclear Corporation  
5 New Street  
White Plains, New York  
Attn: Librarian  
Attn: Mr. Albert Weinstein



Universal Cyclops Steel Corp.  
Refractomet Division  
Bridgeville, Pennsylvania  
Attn: C. P. Mueller

TRW Space Technology Laboratories  
One Space Park  
Redondo Beach, California  
Attn: Librarian

University of California  
Lawrence Radiation Lab.  
P. O. Box 808  
Livermore, California  
Attn: Librarian

University of Michigan  
Department of Chemical & Metallurgical Eng.  
Ann Arbor, Michigan  
Attn: Librarian

Vought Astronautics  
P. O. Box 5907  
Dallas 22, Texas  
Attn: Librarian

Wolverine Tube Division  
Calumet & Hecla, Inc.  
17200 Southfield Road  
Allen Park, Michigan  
Attn: R. C. Cash

Wyman-Gordon Co.  
North Grafton, Massachusetts  
Attn: Librarian

Wah Chang Corporation  
Albany, Oregon  
Attn: Librarian